TABLE 2. Drug susceptibility against HIV clinical isolates in MAGI and NCK45-β-Gal/SEAP cells

Compound	Cell line	Detection	EC_{50} (μM)[a]					
			KMT/R5X4	IVR405/R5X4	IVR406/R5X4	IVR409/R5X4	IVR416/R5X4	IVR417/R5
DS5000	MAGI	β-Gal	0.54	0.43	0.18	0.51	0.16	1.4
	NCK45-β-Gal/SEAP	β-Gal	0.6	0.22	0.14	0.46	0.22	1.9
		SEAP	0.28	0.27	0.19	0.28	0.16	1.5
AZT	MAGI	β-Gal	0.0027	>1.0	0.68	0.055	0.046	0.0033
	NCK45-β-Gal/SEAP	β-Gal	0.0038	>1.0	1.0	0.061	0.018	0.004
		SEAP	0.0044	>1.0	0.41	0.032	0.013	0.0015
ddC	MAGI	β-Gal	1.3	0.55	1.4	1.2	1.0	1.3
	NCK45-β-Gal/SEAP	β-Gal	1.0	0.32	1.0	1.3	0.75	0.79
		SEAP	2.0	0.24	2.1	1.5	0.52	0.77

[a] EC_{50}, 50% antiviral effective concentration. Amino acid substitutions in the RT region were as follows: none for KMT, M41L/E44D/D67G/V118I/Q151M/L210W/T215Y for IVR405, M41L/E44D/D67N/V118I/M184I/L210W/T215Y for IVR406, M41L/E44D/M184V/L210W/T215Y for IVR416, and D67N/V106AV/M184V/T215F for IVR407. Coreceptor usage is indicated in each subheading after the slash: R5X4, CCR5 and CXCR4 dualtropic virus; R5, CCR5-tropic virus.

ical isolates used in the present study were kindly provided by Y. Maeda (Kumamoto University School of Medicine, Kumamoto, Japan) and S. Oka (AIDS Clinical Center, International Medical Center of Japan, Tokyo, Japan). The drug susceptibilities of not only R5-tropic isolates but also X4-tropic and dualtropic isolates were comparable to those in the MAGI assay (Table 2). IVR405 and IVR406 were highly resistant to AZT, whereas IVR409 and IVR416 showed moderate resistance to AZT, and KMT and IVR417 were susceptible to AZT. These susceptibilities were confirmed by the MAGI assay.

In the present study, we established an IRES-mediated tandem-reporter assay using NCK45 cells for the rapid and simultaneous evaluation of the antiviral activities of compounds. This assay enables the evaluation of various HIV strains and clinical isolates within 3 days, including the cell preparation procedure. Secreted SEAP from HIV-infected NCK45 cells is also useful for monitoring the isolation of viruses without cell destruction and enables the continuous propagation of the isolates during isolation. Since NCK45-β-Gal/SEAP cells are susceptible to various viruses, including clinical strains, depending on the experimental purpose any HIV variants may be used for a reference virus, e.g., an isolate prior to the therapy. The LTR promoter for the dual reporters used in the present study includes four CpG methylation-sensitive sites, although Tat can transactivate the HIV-1 LTR regardless of the methylation state (3, 28). Thus, reporter genes in NCK45 cells are less affected by gene silencing.

Compared to the commercially available phenotypic assays, our established system may be useful especially for inhibitors targeting new molecules, including envelope proteins and integrase. A fusion inhibitor T-20 can suppress variants refractory to most of approved RT and protease inhibitors (22, 23). Both phenotypic and genotypic assays for T-20 are needed to evaluate the clinical outcome of patients with T-20-containing regimens. An approved CCR5 antagonist, maraviroc, may also suppress such refractory variants (8). Needless to say, to assess the drug susceptibility experimentally and/or clinically, a combination of established databases accumulated with various assays appears to be useful and important.

In conclusion, the tandem reporters β-Gal and SEAP can evaluate the exact viral infectivity and proportional LTR activation level by repetitive analyses of culture supernatants, respectively. This IRES-mediated tandem-reporter system may be applicable to other reporter genes, e.g., the luciferase gene. Thus, our assay system may provide simple, rapid and stable results for HIV phenotypic assays.

We thank J. Overbaugh for providing the HeLa-CD4/CCR5-LTR/β-Gal cells through the AIDS Research and Reference Reagent Program, Division of AIDS, National Institute of Allergy and Infectious Diseases (Bethesda, MD).

This study was supported in part by a grant for the Promotion of AIDS Research from the Ministry of Health and Welfare of Japan (to M.M. and E.K.); a grant for Research for Health Science Focusing on Drug Innovation from the Japan Health Science Foundation (to E.K.); and a grant from the Ministry of Education, Culture, Sports, Science, and Technology of Japan (to E.K.). K.K. and T.N. are supported by the 21st Century COE Program of the Ministry of Education, Culture, Sports, Science, and Technology.

REFERENCES

1. **Baba, M., O. Nishimura, N. Kanzaki, M. Okamoto, H. Sawada, Y. Iizawa, M. Shiraishi, Y. Aramaki, K. Okonogi, Y. Ogawa, K. Meguro, and M. Fujino.** 1999. A small-molecule, nonpeptide CCR5 antagonist with highly potent and selective anti-HIV-1 activity. Proc. Natl. Acad. Sci. USA 96:5698–5703.
2. **Baldwin, C. E., and B. Berkhout.** 2006. Second site escape of a T20-dependent HIV-1 variant by a single amino acid change in the CD4 binding region of the envelope glycoprotein. Retrovirology 3:84.
3. **Bednarik, D. P., J. A. Cook, and P. M. Pitha.** 1990. Inactivation of the HIV LTR by DNA CpG methylation: evidence for a role in latency. EMBO J. 9:1157–1164.
4. **Brann, T. W., R. L. Dewar, M. K. Jiang, A. Shah, K. Nagashima, J. A. Metcalf, J. Falloon, H. C. Lane, and T. Imamichi.** 2006. Functional correlation between a novel amino acid insertion at codon 19 in the protease of human immunodeficiency virus type 1 and polymorphism in the p1/p6 Gag cleavage site in drug resistance and replication fitness. J. Virol. 80:6136–6145.
5. **Brehm, J. H., D. Koontz, J. D. Meteer, V. Pathak, N. Sluis-Cremer, and J. W. Mellors.** 2007. Selection of mutations in the connection and RNase H domains of human immunodeficiency virus type 1 reverse transcriptase that increase resistance to 3′-azido-3′-dideoxythymidine. J. Virol. 81:7852–7859.
6. **Cabrera, C., S. Marfil, E. Garcia, J. Martinez-Picado, A. Bonjoch, M. Bofill, S. Moreno, E. Ribera, P. Domingo, B. Clotet, and L. Ruiz.** 2006. Genetic evolution of gp41 reveals a highly exclusive relationship between codons 36, 38, and 43 in gp41 under long-term enfuvirtide-containing salvage regimen. Aids 20:2075–2080.
7. **Delviks-Frankenberry, K. A., G. N. Nikolenko, R. Barr, and V. K. Pathak.** 2007. Mutations in human immunodeficiency virus type 1 RNase H primer grip enhance 3′-azido-3′-deoxythymidine resistance. J. Virol. 81:6837–6845.
8. **Fatkenheuer, G., A. L. Pozniak, M. A. Johnson, A. Plettenberg, S. Staszewski, A. I. Hoepelman, M. S. Saag, F. D. Goebel, J. K. Rockstroh, B. J. Dezube, T. M. Jenkins, C. Medhurst, J. F. Sullivan, C. Ridgway, S. Abel, I. T. James, M. Youle, and E. van der Ryst.** 2005. Efficacy of short-term monotherapy

with maraviroc, a new CCR5 antagonist, in patients infected with HIV-1. Nat. Med. 11:1170–1172.
9. **Frenkel, L. M., L. E. Wagner II, S. M. Atwood, T. J. Cummins, and S. Dewhurst.** 1995. Specific, sensitive, and rapid assay for human immunodeficiency virus type 1 *pol* mutations associated with resistance to zidovudine and didanosine. J. Clin. Microbiol. 33:342–347.
10. **Gao, W. Y., R. Agbaria, J. S. Driscoll, and H. Mitsuya.** 1994. Divergent anti-human immunodeficiency virus activity and anabolic phosphorylation of 2',3'-dideoxynucleoside analogs in resting and activated human cells. J. Biol. Chem. 269:12633–12638.
11. **Hachiya, A., S. Aizawa-Matsuoka, M. Tanaka, Y. Takahashi, S. Ida, H. Gatanaga, Y. Hirabayashi, A. Kojima, M. Tatsumi, and S. Oka.** 2001. Rapid and simple phenotypic assay for drug susceptibility of human immunodeficiency virus type 1 using CCR5-expressing HeLa/CD4$^+$ cell clone 1-10 (MAGIC-5). Antimicrob. Agents Chemother. 45:495–501.
12. **Hachiya, A., H. Gatanaga, E. Kodama, M. Ikeuchi, M. Matsuoka, S. Harada, H. Mitsuya, S. Kimura, and S. Oka.** 2004. Novel patterns of nevirapine resistance-associated mutations of human immunodeficiency virus type 1 in treatment-naive patients. Virology 327:215–224.
13. **Hanna, G. J., and R. T. D'Aquila.** 2001. Clinical use of genotypic and phenotypic drug resistance testing to monitor antiretroviral chemotherapy. Clin. Infect. Dis. 32:774–782.
14. **Hertogs, K., M. P. de Bethune, V. Miller, T. Ivens, P. Schel, A. Van Cauwenberge, C. Van Den Eynde, V. Van Gerwen, H. Azijn, M. Van Houtte, F. Peeters, S. Staszewski, M. Conant, S. Bloor, S. Kemp, B. Larder, and R. Pauwels.** 1998. A rapid method for simultaneous detection of phenotypic resistance to inhibitors of protease and reverse transcriptase in recombinant human immunodeficiency virus type 1 isolates from patients treated with antiretroviral drugs. Antimicrob. Agents Chemother. 42:269–276.
15. **Jang, S. K., and E. Wimmer.** 1990. Cap-independent translation of encephalomyocarditis virus RNA: structural elements of the internal ribosomal entry site and involvement of a cellular 57-kD RNA-binding protein. Genes Dev. 4:1560–1572.
16. **Jones, S., and M. E. Klotman.** 2001. Impact of genotypic resistance testing on physician selection of antiretroviral therapy. J. Hum. Virol. 4:214–216.
17. **Kajiwara, K., E. Kodama, and M. Matsuoka.** 2006. A novel colorimetric assay for CXCR4 and CCR5 tropic human immunodeficiency viruses. Antivir. Chem. Chemother. 17:215–223.
18. **Kellam, P., and B. A. Larder.** 1994. Recombinant virus assay: a rapid, phenotypic assay for assessment of drug susceptibility of human immunodeficiency virus type 1 isolates. Antimicrob. Agents Chemother. 38:23–30.
19. **Ketas, T. J., S. E. Kuhmann, A. Palmer, J. Zurita, W. He, S. K. Ahuja, P. J. Klasse, and J. P. Moore.** 2007. Cell surface expression of CCR5 and other host factors influence the inhibition of HIV-1 infection of human lymphocytes by CCR5 ligands. Virology 364:281–290.
20. **Kimpton, J., and M. Emerman.** 1992. Detection of replication-competent and pseudotyped human immunodeficiency virus with a sensitive cell line on the basis of activation of an integrated β-galactosidase gene. J. Virol. 66: 2232–2239.
21. **Korn, K., H. Reil, H. Walter, and B. Schmidt.** 2003. Quality control trial for human immunodeficiency virus type 1 drug resistance testing using clinical samples reveals problems with detecting minority species and interpretation of test results. J. Clin. Microbiol. 41:3559–3565.
22. **Lalezari, J. P., K. Henry, M. O'Hearn, J. S. Montaner, P. J. Piliero, B. Trottier, S. Walmsley, C. Cohen, D. R. Kuritzkes, J. J. Eron, Jr., J. Chung, R. DeMasi, L. Donatacci, C. Drobnes, J. Delehanty, and M. Salgo.** 2003. Enfuvirtide, an HIV-1 fusion inhibitor, for drug-resistant HIV infection in North and South America. N. Engl. J. Med. 348:2175–2185.
23. **Lazzarin, A., B. Clotet, D. Cooper, J. Reynes, K. Arasteh, M. Nelson, C. Katlama, H. J. Stellbrink, J. F. Delfraissy, J. Lange, L. Huson, R. DeMasi, C. Wat, J. Delehanty, C. Drobnes, and M. Salgo.** 2003. Efficacy of enfuvirtide in patients infected with drug-resistant HIV-1 in Europe and Australia. N. Engl. J. Med. 348:2186–2195.
24. **Loutfy, M. R., J. M. Raboud, J. S. Montaner, T. Antoniou, B. Wynhoven, F. Smaill, D. Rouleau, J. Gill, W. Schlech, Z. L. Brumme, T. Mo, K. Gough, A. Rachlis, P. R. Harrigan, and S. L. Walmsley.** 2007. Assay of HIV gp41 amino acid sequence to identify baseline variation and mutation development in patients with virologic failure on enfuvirtide. Antivir. Res. 75:58–63.
25. **Maguire, M. F., R. Guinea, P. Griffin, S. Macmanus, R. C. Elston, J. Wolfram, N. Richards, M. H. Hanlon, D. J. Porter, T. Wrin, N. Parkin, M. Tisdale, E. Furfine, C. Petropoulos, B. W. Snowden, and J. P. Kleim.** 2002. Changes in human immunodeficiency virus type 1 Gag at positions L449 and P453 are linked to I50V protease mutants in vivo and cause reduction of sensitivity to amprenavir and improved viral fitness in vitro. J. Virol. 76:7398–7406.
26. **Nikolenko, G. N., K. A. Delviks-Frankenberry, S. Palmer, F. Maldarelli, M. J. Fivash, Jr., J. M. Coffin, and V. K. Pathak.** 2007. Mutations in the connection domain of HIV-1 reverse transcriptase increase 3'-azido-3'-deoxythymidine resistance. Proc. Natl. Acad. Sci. USA 104:317–322.
27. **Perez-Alvarez, L., R. Carmona, A. Ocampo, A. Asorey, C. Miralles, S. Perez de Castro, M. Pinilla, G. Contreras, J. A. Taboada, and R. Najera.** 2006. Long-term monitoring of genotypic and phenotypic resistance to T20 in treated patients infected with HIV-1. J. Med. Virol. 78:141–147.
28. **Pion, M., A. Jordan, A. Biancotto, F. Dequiedt, F. Gondois-Rey, S. Rondeau, R. Vigne, J. Hejnar, E. Verdin, and I. Hirsch.** 2003. Transcriptional suppression of in vitro-integrated human immunodeficiency virus type 1 does not correlate with proviral DNA methylation. J. Virol. 77:4025–4032.
29. **Reeves, J. D., S. A. Gallo, N. Ahmad, J. L. Miamidian, P. E. Harvey, M. Sharron, S. Pohlmann, J. N. Sfakianos, C. A. Derdeyn, R. Blumenthal, E. Hunter, and R. W. Doms.** 2002. Sensitivity of HIV-1 to entry inhibitors correlates with envelope/coreceptor affinity, receptor density, and fusion kinetics. Proc. Natl. Acad. Sci. USA 99:16249–16254.
30. **Rhee, S. Y., J. Taylor, G. Wadhera, A. Ben-Hur, D. L. Brutlag, and R. W. Shafer.** 2006. Genotypic predictors of human immunodeficiency virus type 1 drug resistance. Proc. Natl. Acad. Sci. USA 103:17355–17360.
31. **Richman, D. D.** 2000. Principles of HIV resistance testing and overview of assay performance characteristics. Antivir. Ther. 5:27–31.
32. **Salomon, H., A. Belmonte, K. Nguyen, Z. Gu, M. Gelfand, and M. A. Wainberg.** 1994. Comparison of cord blood and peripheral blood mononuclear cells as targets for viral isolation and drug sensitivity studies involving human immunodeficiency virus type 1. J. Clin. Microbiol. 32:2000–2002.
33. **Sarmati, L., E. Nicastri, S. G. Parisi, G. d'Ettorre, G. Mancino, P. Narciso, V. Vullo, and M. Andreoni.** 2002. Discordance between genotypic and phenotypic drug resistance profiles in human immunodeficiency virus type 1 strains isolated from peripheral blood mononuclear cells. J. Clin. Microbiol. 40:335–340.
34. **Shafer, R. W., M. J. Kozal, D. A. Katzenstein, W. H. Lipil, I. F. Johnstone, and T. C. Merigan.** 1993. Zidovudine susceptibility testing of human immunodeficiency virus type 1 (HIV) clinical isolates. J. Virol. Methods 41:297–310.
35. **Shi, C., and J. W. Mellors.** 1997. A recombinant retroviral system for rapid in vivo analysis of human immunodeficiency virus type 1 susceptibility to reverse transcriptase inhibitors. Antimicrob. Agents Chemother. 41:2781–2785.
36. **Soda, Y., N. Shimizu, A. Jinno, H. Y. Liu, K. Kanbe, T. Kitamura, and H. Hoshino.** 1999. Establishment of a new system for determination of coreceptor usages of HIV based on the human glioma NP-2 cell line. Biochem. Biophys. Res. Commun. 258:313–321.
37. **Tamamura, H., Y. Xu, T. Hattori, X. Zhang, R. Arakaki, K. Kanbara, A. Omagari, A. Otaka, T. Ibuka, N. Yamamoto, H. Nakashima, and N. Fujii.** 1998. A low-molecular-weight inhibitor against the chemokine receptor CXCR4: a strong anti-HIV peptide T140. Biochem. Biophys. Res. Commun. 253:877–882.

JOURNAL OF VIROLOGY, Jan. 2008, p. 764–774
0022-538X/08/$08.00+0 doi:10.1128/JVI.01534-07

Vol. 82, No. 2

Broad Antiretroviral Activity and Resistance Profile of the Novel Human Immunodeficiency Virus Integrase Inhibitor Elvitegravir (JTK-303/GS-9137)▽†

Kazuya Shimura,[1] Eiichi Kodama,[1]* Yasuko Sakagami,[1] Yuji Matsuzaki,[2] Wataru Watanabe,[2]‡ Kazunobu Yamataka,[2] Yasuo Watanabe,[2] Yoshitsugu Ohata,[2] Satoki Doi,[3] Motohide Sato,[2] Mitsuki Kano,[2] Satoru Ikeda,[2] and Masao Matsuoka[1]

Laboratory of Virus Immunology, Institute for Virus Research, Kyoto University, 53 Kawaramachi, Shogoin, Sakyo-ku, Kyoto 606-8507, Japan[1]; Japan Tobacco Inc., Central Pharmaceutical Research Institute, 1-1 Murasaki-cho, Takatsuki, Osaka 569-1125, Japan[2]; and Japan Tobacco Inc., Central Pharmaceutical Research Institute, Pharmaceutical Frontier Research Laboratories, 1-13-2 Fukuura, Kanazawa-Ku, Yokohama, Kanagawa 236-0004, Japan[3]

Received 13 July 2007/Accepted 22 October 2007

Integrase (IN), an essential enzyme of human immunodeficiency virus (HIV), is an attractive antiretroviral drug target. The antiviral activity and resistance profile in vitro of a novel IN inhibitor, elvitegravir (EVG) (also known as JTK-303/GS-9137), currently being developed for the treatment of HIV-1 infection are described. EVG blocked the integration of HIV-1 cDNA through the inhibition of DNA strand transfer. EVG inhibited the replication of HIV-1, including various subtypes and multiple-drug-resistant clinical isolates, and HIV-2 strains with a 50% effective concentration in the subnanomolar to nanomolar range. EVG-resistant variants were selected in two independent inductions, and a total of 8 amino acid substitutions in the catalytic core domain of IN were observed. Among the observed IN mutations, T66I and E92Q substitutions mainly contributed to EVG resistance. These two primary resistance mutations are located in the active site, and other secondary mutations identified are proximal to these primary mutations. The EVG-selected IN mutations, some of which represent novel IN inhibitor resistance mutations, conferred reduced susceptibility to other IN inhibitors, suggesting that a common mechanism is involved in resistance and potential cross-resistance. The replication capacity of EVG-resistant variants was significantly reduced relative to both wild-type virus and other IN inhibitor-resistant variants selected by L-870,810. EVG and L-870,810 both inhibited the replication of murine leukemia virus and simian immunodeficiency virus, suggesting that IN inhibitors bind to a conformationally conserved region of various retroviral IN enzymes and are an ideal drug for a range of retroviral infections.

Three unique and essential HIV enzymes, protease (PR), reverse transcriptase with RNase H (RT), and integrase (IN), appear to be ideal targets for the development of inhibitors of human immunodeficiency virus (HIV) replication. Anti-HIV drugs targeting PR (PR inhibitors [PIs]) and RT (nucleoside/nucleotide RT inhibitors [NRTIs] and nonnucleoside RT inhibitors [NNRTIs]) have been approved for use in the treatment of HIV infection. Combinations of these drugs used in highly active antiretroviral therapy can effectively suppress HIV replication in vivo to undetectable levels and have led to significant declines in HIV-associated mortality (28, 40). However, the emergence of drug-resistant HIV variants can attenuate the efficacy of antiretroviral treatment. Some primary infections also result from the transmission of HIV strains that possess drug-resistant genotypes and phenotypes (9). To suppress these drug-resistant variants, new anti-HIV drugs that block new targets are urgently needed.

IN, a 32-kDa protein resulting from the proteolytic cleavage of the *gag-pol* precursor, plays an essential role in the integration of proviral DNA into the host genome. As LaFemina et al. previously reported that there is no human homologue of HIV IN (31), it is an attractive target for the development of new antiretroviral therapeutic agents without adverse effects. IN consists of three domains: an N-terminal zinc finger domain and a C-terminal DNA-binding domain flank a central catalytic core domain (CCD) that plays a critical role in its enzymatic activity (13, 14). Following reverse transcription, IN exerts at least two functions: the cleavage of two conserved nucleotides from the 3′ ends of both strands of the viral cDNA (3′ processing) (1) and, subsequently, the ligation of the viral cDNA into the host genome (strand transfer) (14). Gap filling of the interfaces between the viral and host genomic DNA is then completed using the host DNA repair machinery via a mechanism that is not yet fully understood. The completion of integration results in a fully functional provirus, which can then be used to initiate viral DNA transcription.

Several compounds that inhibit IN activity have been described, including diketo acid (DKA) derivatives such as L-731,988 (24) and S-1360 (16), both of which have potent

* Corresponding author. Mailing address: Laboratory of Virus Immunology, Institute for Virus Research, Kyoto University, 53 Kawaramachi, Shogoin, Sakyo-ku, Kyoto 606-8507, Japan. Phone and fax: 81-75-751-3986. E-mail: ekodama@virus.kyoto-u.ac.jp.

† Supplemental material for this article may be found at http://jvi.asm.org/.

‡ Present address: Kyushu University of Health and Welfare, 1714-1 Yoshinomachi, Nobeoka, Miyazaki 882-8508, Japan.

▽ Published ahead of print on 31 October 2007.

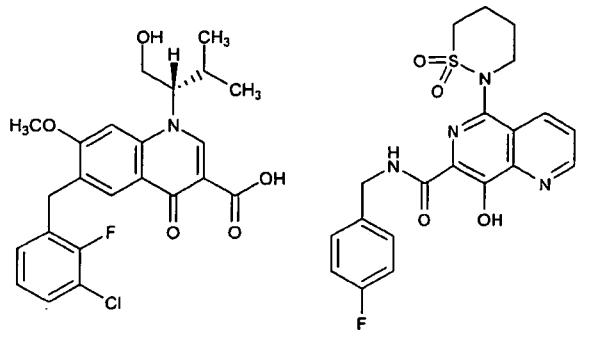

elvitegravir (EVG) L-870,810

FIG. 1. Structure of EVG and L-870,810. A dihydroquinoline carboxylic acid derivative, EVG, and a naphthyridine carboxamide derivative, L-870,810 (a representative IN inhibitor), are shown.

antiviral activity. Crystal structure analysis has indicated that 1-(5-chloroindol-3-yl)-3-hydroxy-3-(2*H*-tetrazol-5-yl)-propenone, an S-1360 derivative, binds to the CCD, the putative active site of IN (19). In vitro resistance selection experiments with several IN inhibitors demonstrated that mutations in the CCD of IN play a significant role in the generation of IN inhibitor-resistant viral variants. In vitro selection of HIV-1 in the presence of the DKA IN inhibitors L-731,988 and S-1360 resulted in the emergence of viral variants carrying IN mutations associated with resistance. These mutations, including T66I, S153Y, and M154I, are located in close proximity to the catalytic triad residues (D64, D116, and E152) in the CCD of IN (16, 24). In contrast, L-870,810 (Fig. 1), which has previously demonstrated potent antiviral activity in HIV-1-infected patients in a monotherapy study (33), induced unique IN mutations, including V72I, F121Y, T125K, and V151I, when HIV was selected with the compound in vitro (23). These mutations are also located in the active site of IN, suggesting that a common mechanism may be involved in the acquisition of resistance to IN inhibitors.

Although no IN inhibitors are currently approved for clinical use (41), two IN inhibitors, elvitegravir (EVG) (formerly known as JTK-303/GS-9137, being codeveloped by Gilead Sciences and Japan Tobacco) (Fig. 1) (43, 56) and raltegravir (MK-0518, developed by Merck) (22), are currently being investigated in clinical studies of HIV-1-infected patients. In a phase II study, antiretroviral treatment-experienced patients using 125 mg EVG (boosted with ritonavir) along with an active optimized background regimen showed >2-$\log_{10}$ declines in their viral loads that were durable through week 24 (56).

Here, we describe the antiviral activity, mechanism of action, and resistance profile of EVG in vitro. EVG exerted potent anti-HIV activity against not only wild-type strains but also drug-resistant clinical isolates. Interestingly, EVG also showed antiviral activity against murine leukemia virus (MLV) and simian immunodeficiency virus (SIV). These results imply that IN inhibitors are ideal agents for the treatment of a range of retroviral infections. During the selection of EVG-resistant viral variants, novel IN mutations emerged. Combinations of these mutations conferred resistance to EVG and reduced susceptibility to other IN inhibitors, suggesting that there is a common mechanism underlying the resistance to IN inhibitors. One such mechanism may be conformational changes induced by multiple mutations located in the active site of IN.

MATERIALS AND METHODS

Antiviral agents. Zidovudine (AZT) and dextran sulfate (DS5000) (average molecular weight, 5,000) were purchased from Sigma (St. Louis, MO). Efavirenz (EFV) (NNRTI) and nelfinavir (NFV) (PI) were used for the control inhibitor. EVG (43), L-731,988 (42), L-870,810 (23), and S-1360 (16) were synthesized as described previously. The structures of EVG and L-870,810 are depicted in Fig. 1.

Cells and viruses. MT-2 and MT-4 cells were grown in RPMI 1640 medium. 293T cells were grown in Dulbecco's modified Eagle's medium. These media were supplemented with 10% fetal calf serum, 2 mM L-glutamine, 100 U/ml penicillin, and 50 μg/ml streptomycin. HeLa-CD4/CCR5-LTR/β-gal cells (5) were kindly provided by J. Overbaugh through the AIDS Research and Reference Reagent Program, Division of AIDS, National Institute of Allergy and Infectious Diseases (Bethesda, MD), and maintained in Dulbecco's modified Eagle's medium supplemented with 10% fetal calf serum, 200 μg/ml hygromycin B, 10 μg/ml puromycin, and 200 μg/ml geneticin. Peripheral blood mononuclear cells (PBMC) were obtained from healthy HIV-1-seronegative donors by centrifugation through Ficoll-Hypaque density gradients. PBMC were stimulated with 20 U/ml interleukin-2 (Shionogi, Osaka, Japan) and 0.5 μg/ml phytohemagglutinin (Sigma) for 3 days and then used for assays as described previously (30).

Three laboratory strains, HIV-1_{IIIB}, HIV-2_{EHO}, and HIV-2_{ROD}, were used in this study. Various subtypes of drug-naïve clinical isolates of HIV-1 (four isolates of subtype B and seven isolates of non-B subtypes) were employed. Four drug-resistant clinical isolates of HIV-1, including IVR401, IVR409, IVR411, and IVR415, were kindly provided by S. Oka (AIDS Clinical Center, International Medical Center of Japan, Tokyo, Japan).

Determination of HIV drug susceptibility. Inhibitory effects of compounds on HIV infection were determined using multinuclear activation of a galactosidase indicator (MAGI) assay, as previously described (37). Inhibitory effects on HIV-1 clinical isolates were measured by p24 production, and cytotoxicity was measured by using a 3-(4,5-dimethylthiazol-2-yl)-2,5-diphenyltetrazolium bromide (MTT) colorimetric assay, as described previously (30). Antiviral activities and cytotoxicities of inhibitors are presented as the concentrations that block viral replication by 50% (50% effective concentration [EC_{50}]) and that suppress the viability of target cells by 50%, respectively.

Quantification of HIV-1 DNA species. MT-2 cells (5×10^5 cells) were infected with HIV-1_{IIIB} at a multiplicity of infection (MOI) of 0.1 in the absence or presence of various inhibitors. Infected cells were washed after incubation for 2 h at 37°C. At 24 h postinfection, DNA was extracted using DNAzol reagent (Invitrogen, Carlsbad, CA).

Quantification of integrated HIV-1 DNA and the two-long-terminal-repeat (2-LTR) circle was performed by real-time quantitative PCR as described previously (4). To normalize DNA species among inhibitors, β-globin amplification was used as an internal control (51). Reactions were analyzed by using the ABI Prism 7500 sequence detector (PE Applied Biosystems, Foster City, CA), and results were then normalized and expressed as relative HIV-1 DNA species compared to a "no-inhibitor" control.

In vitro strand transfer assay. An oligonucleotide-based strand transfer assay was performed as previously described (8), with some modifications. Briefly, preprocessed oligonucleotide H-U5V1-2 (5'-ATGTGGAAAATCTCTAGCA-3'), derived from the U5 end of the HIV-1 LTR, was labeled at the 5' end with [γ-^{32}P]ATP. Radiolabeled H-U5V1-2 was annealed to H-U5V2 (5'-ACTGCTA GAGATTTTCCACAT-3') and then used for assays. Recombinant HIV-1 IN derived from HIV-1 NL4-3 (wild type) or EVG-selected mutants was prepared using an *Escherichia coli* expression system. The strand transfer assay was performed with 1 μM IN and 150 nM substrate DNA in 20 mM MOPS (morpholinepropanesulfonic acid) buffer with 30 mM $MgCl_2$ incubated in either the presence or absence of IN inhibitors at 37°C for 60 min. Reaction products were analyzed by electrophoresis on 25% polyacrylamide gels and quantified using a BAS-2500 imaging system (Fuji Photo Film, Tokyo, Japan). The concentration of IN inhibitor that inhibited the production of strand transfer products by 50% (50% inhibitory concentration [IC_{50}]) compared to the control was determined.

Selection of EVG-resistant HIV-1 variants in vitro. MT-2 cells (2×10^5 cells) were infected with HIV-1_{IIIB} and then cultured in the presence of 0.5 nM (see Fig. 3A) or 0.1 nM (see Fig. 3B) EVG. Cultures were incubated at 37°C until an

TABLE 1. Antiviral activities against laboratory HIV strains[a]

Strain	Mean EC_{50} (nM) ± SD		
	AZT	EVG	L-870,810
HIV-1_{IIIB}	7.1 ± 1.3	0.7 ± 0.3	6.3 ± 0.3
HIV-2_{EHO}	22 ± 9.1	2.8 ± 0.8	11 ± 1.9
HIV-2_{ROD}	19 ± 4.7	1.4 ± 0.7	8.6 ± 0.4

[a] Antiviral activity was determined using the MAGI assay. Data shown are means and standard deviations obtained from at least three independent experiments.

extensive cytopathic effect (CPE) was observed, and the culture supernatant was then harvested for further passage in fresh MT-2 cells. The concentration of EVG was increased when a significant CPE was observed. At the indicated passages (see Fig. 3A and B), proviral DNA was extracted from infected MT-2 cells and then subjected to PCR, followed by direct population-based sequencing. Susceptibility to EVG at the indicated passages was determined using the MAGI assay (see Fig. 3A) or p24 production (see Fig. 3B).

Recombinant HIV-1 clones. An HIV-1 infectious clone, pNL101 (38), kindly provided by K.-T. Jeang (NIH, Bethesda, MD), was used to generate recombinant HIV-1 clones. Wild-type HIV-1 (HIV-1_{WT}) was constructed by replacing the *pol* coding region (nucleotide positions 2006 of the ApaI site to 5122 of the NdeI site of pNL101) with HIV-1 strain BH10. The *pol* coding region contains a silent mutation at nucleotide 4232 (TTTAGA to TCTAGA) resulting in the generation of a unique XbaI site. Recombinant HIV-1 IN infectious clones were generated using a modified pNL101-based vector, $pNLRT_{WT}$. In brief, mutations were introduced into the XbaI-NdeI region (891 bp) of $pSLInt_{WT}$, which encodes nucleotides 4232 to 5122 of pNL101, using an oligonucleotide-based site-directed mutagenesis method (54). Next, the XbaI-NdeI fragments were inserted into pBNΔInt, which encodes nucleotides 5122 (NdeI) to 5785 (SalI) of pNL101. Finally, the XbaI-SalI region (1,554 bp) was inserted into pNL101. Each infectious clone was transfected into 293T cells. The following day, MT-2 cells were added, and the supernatants were harvested when an extensive CPE was observed.

Replication kinetics of resistant HIV-1 variants. MT-2 cells (10^5 cells) were infected with each virus preparation (500 MAGI units) for 4 h. The infected cells were then washed and cultured in the presence or absence of EVG. The culture supernatants were harvested on day 5 after infection, and p24 levels were quantified using a Retro-Tek HIV-1 p24 antigen enzyme-linked immunosorbent assay (ELISA) (ZeptoMetrix, Buffalo, NY).

Evaluation of antiretroviral activities of IN inhibitors. The MLV-based retroviral vector pRCV/LIG (15) and plasmid pcDNA-VSVG, encoding the vesicular stomatitis virus envelope glycoprotein (a generous gift from H. Miyoshi, RIKEN Bioresource Center, Tsukuba, Japan), were employed to generate viral particles. These plasmids were cotransfected into an MLV-derived Gag-Pol-expressing packaging cell line, GP293 (Clontech, Palo Alto, CA). After 48 h of transfection, culture supernatants were filtered through a 0.45-μm membrane and stored at −80°C until use.

An HIV-1-based luciferase expression vector, pBC-LIG; pCMVΔ8/9, encoding the HIV-1 viral proteins including IN; and pcDNA-VSVG were transfected into 293T cells to generate pseudotyped HIV-1. The viruses were used to infect 293T cells (10^5 cells per well in 12-well plates) at an MOI of 0.02 in the absence or presence of inhibitors. After 48 h of transduction, luciferase activity was determined using a luciferase assay system (Promega, Madison, WI) and an LB 9507 luminometer (Berthold, Bad Wildbad, Germany).

An SIV molecular clone, pMA239 (46), containing the full SIVmac239 genome, was a kind gift from E. Ido, Institute for Virus Research, Kyoto University. pMA239 was used to generate viral stocks as previously described (6). Antiviral activities of IN inhibitors against SIVmac239 were determined using the MAGI assay as described above.

Molecular modeling studies. A three-dimensional model of EVG in complex with HIV-1 IN CCD was prepared by PyMOL software, version 0.97, using previously reported data (44). Amino acid residues involved in resistance to EVG were displayed within this model.

RESULTS

Anti-HIV activities of IN inhibitors. The antiviral activity of EVG against HIV-1_{IIIB}, HIV-2_{EHO}, and HIV-2_{ROD} was first evaluated by the MAGI assay. EVG showed potent antiviral activity against three laboratory strains of HIV, with EC_{50} values in the subnanomolar to nanomolar range (Table 1). Next, we evaluated the activity of EVG against wild-type clinical isolates representing various subtypes of HIV-1. EVG suppressed the replication of all HIV-1 subtypes tested, with an antiviral EC_{50} ranging from 0.10 to 1.26 nM (Table 2). Moreover, EVG suppressed the replication of HIV-1 clinical isolates carrying NRTI, NNRTI, and PI resistance-associated genotypes, as did a control IN inhibitor, the compound L-870,810 (see Table S1 in the supplemental material). The cytotoxicities of these inhibitors were also determined using an MTT colorimetric assay. Mean values for the concentration that suppresses the viability of target cells by 50% for EVG and L-870,810 in PBMC obtained from three independent donors were 4.6 ± 0.5 μM and 2.7 ± 0.6 μM, respectively. Thus, EVG can suppress various HIV strains, including diverse HIV-1 subtypes and clinical isolates carrying multiple mutations associated with resistance to currently approved antiretroviral drugs.

TABLE 2. Antiviral activities of EVG against various subtypes of HIV-1[a]

Subtype	Isolate	EC_{50} (nM)	
		AZT	EVG
A	RW/92/016	7.91	0.41
B	96USHIPS7	8.41	0.26
	BR/92/021	2.13	0.76
	BR/93/017	1.10	0.18
	BR/93/022	11.7	1.13
C	BR/92/025	2.84	0.10
D	UG/92/046	7.26	0.50
E	CMU02	9.07	1.26
F	BR/93/020	25.3	0.74
G	JV1083	11.1	0.35
O	BCF01	1.52	1.17

[a] Antiviral activity was determined using p24 ELISA.

Mechanism of anti-HIV activity of EVG. First, we performed a "time-of-addition" experiment as described previously (30), with some modifications. MT-4 cells were infected with HIV-1_{IIIB} at an MOI of 0.5. One hour after infection, infected cells were extensively washed, and compounds were added, including an NNRTI (EFV at 100 nM), a PI (NFV at 500 nM), or EVG (100 nM). Amounts of p24 antigen were determined at 31 h postinfection. The antiviral activity of EFV gradually decreased from 6 h postinfection and disappeared at 12 h postinfection, whereas the antiviral activity of EVG decreased from 10 h postinfection and was no longer detected by 12 h postinfection. On the other hand, the PI NFV effectively blocked the infection up to 12 h postinfection and still exerted approximately 20% inhibitory activity up to 24 h postinfection. These results strongly suggest that EVG inhibits the HIV replication at a step that occurs after reverse transcription but before proteolytic cleavage, consistent with the integration step.

To elucidate the mode of action of EVG on HIV-1 replication, the levels of intracellular HIV-1 DNA species were determined using real-time quantitative PCR (Fig. 2A). MT-2 cells were infected with HIV-1_{IIIB} in the presence or absence

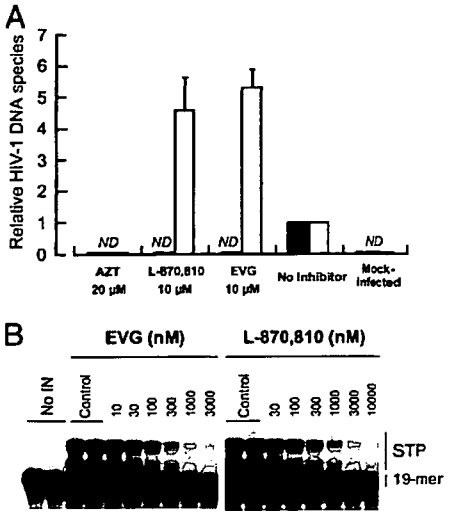

FIG. 2. Mechanism of action of EVG. (A) Quantification of HIV-1 DNA species. MT-2 cells were infected with HIV-1_{IIIB} in the presence or absence of AZT, L-870,810, and EVG. Unintegrated (2-LTR) (white bars) and integrated (black bars) forms of proviral DNA were quantified by real-time PCR and normalized to the β-globin gene after 24 h of infection. The data are represented as means and standard deviations of value relative to that of the no-inhibitor control from three independent experiments. ND means that the signals were not detected even after 40 cycles of amplification. (B) Inhibitory effect of IN inhibitors on strand transfer activity. Gel electrophoresis shows strand transfer products (STP) generated from preprocessed donor DNA substrate (19-mer) covalently bound to acceptor DNA.

of a CD4-gp120 binding inhibitor, DS5000; an NRTI, AZT; an IN inhibitor, L-870,810; and EVG. Unintegrated (2-LTR) and integrated forms of reverse-transcribed HIV-1 genomic DNA were quantified after 24 h of infection and then normalized with β-globin DNA. In the presence of 20 μM AZT, neither 2-LTR nor integrated forms were detected as expected. Similar results were also observed with 20 μM DS5000 (data not shown). In the presence of 10 μM L-870,810, integrated provirus was undetectable, while relative 2-LTR levels increased about 5-fold (4.6-fold ± 1.0-fold). Similar results were observed with 10 μM EVG (2-LTR) (5.3-fold ± 0.5-fold), indicating that EVG exerts anti-HIV activity by blocking the integration step.

To further characterize the mechanism by which EVG inhibits the integration step, the effect of EVG on strand transfer was assessed by characterizing its ability to inhibit the activity of recombinant wild-type HIV-1 IN enzyme in an oligonucleotide-based strand transfer assay (Fig. 2B). EVG and L-870,810 both inhibited the synthesis of strand transfer products with IC_{50} values of 54 nM and 118 nM, respectively. Taken together, these results indicate that like L-870,810, EVG blocks integration via the inhibition of IN-mediated strand transfer.

Selection of EVG-resistant HIV-1 variants in vitro. To determine the in vitro resistance profile of EVG, EVG-resistant viral variants were selected using a dose escalation method, and the susceptibilities of the resulting selected variants to EVG (EC_{50}) were determined. Selection of resistant HIV-1_{IIIB} was initiated with 0.5 nM EVG (Fig. 3A). At passage 12 (P-12), where the concentration of EVG was 4 nM, 2 amino acid substitutions, glutamine-to-proline at IN codon 146 (Q146P) and asparagine-to-aspartic acid at IN codon 232 (N232D), were observed (Fig. 3A). An N232D substitution was previously reported to be an IN polymorphism in HIV-1 (34). The EVG EC_{50} of a P-24 variant containing a Q146P- and N232D-substituted variant was 6.2 nM. At P-32 (32 nM EVG), a T66I IN substitution was newly observed, whereas the N232D substitution had reverted to the baseline sequence. The EVG EC_{50} against a P-36 variant was 64 nM. An S147G IN substitution was detected at P-48 (128 nM EVG), and the EVG EC_{50} further increased to 635 nM. In addition, a Q95Q/K IN substitution (mixture of Q and K) and an E138E/K IN substitution were newly identified at P-54 (256 nM EVG). These mixtures, Q95Q/K and E138E/K, fully emerged in the viral pools by P-64 and P-80, respectively. The EVG EC_{50} at P-68 (1,024 nM EVG) was greater than 1,000 nM.

An independent EVG selection experiment, again using HIV-1_{IIIB}, was performed but began at 0.1 nM EVG (Fig. 3B). An E92E/Q mixture in the IN coding region was first detected at P-30 (10 nM EVG) and was predominantly E92Q by P-38 (20 nM EVG). Additional IN substitutions, H51H/Y and S147S/G, emerged at P-60 (640 nM EVG), and an E157E/Q mixture emerged at P-70 (1,280 nM EVG); the viral pools at the terminal passage P-80 (1,280 nM EVG) had the IN sequence H51Y/E92Q/S147G/E157E/Q (Fig. 3B). The emergence of each of these mutations correlated with an increase in the EVG EC_{50} of the resulting viral pools (Fig. 3). Other than the N232D polymorphism, all of these mutations are located in the CCD of IN.

Phenotypic analysis of IN recombinant viruses. (i) EVG-selected mutations. To characterize which mutations are responsible for EVG resistance, infectious HIV-1 clones containing single IN substitutions (H51Y, T66I, E92Q, Q95K, E138K, Q146P, S147G, or E157Q) that were observed to emerge under selection with EVG were generated (Fig. 3 and Table 3). Mutations were classified into two groups based on the level of resistance: mutations that conferred more than 10-fold reduced susceptibility compared to the wild type were defined as primary mutations, and mutations conferring less than 10-fold reduced susceptibility were defined as secondary mutations. T66I and E92Q substitutions conferred significantly reduced susceptibility to EVG (37- and 36-fold reduced, respectively, relative to the wild type), whereas the Q146P and S147G substitutions conferred more moderate reductions in EVG susceptibility (11-fold reduced), indicating that these four IN mutations are primary mutations involved in resistance to EVG. In contrast, H51Y, Q95K, and E157Q substitutions all conferred smaller reductions in EVG susceptibility (each less than 6.3-fold reduced compared to the wild type), suggesting that these substitutions are secondary resistance mutations. Interestingly, the E138K mutation alone conferred no reduction in susceptibility to either EVG or L-870,810. Thus, several distinct mechanisms of resistance may be represented by these different IN mutations.

Multisubstituted clones observed during EVG selection experiments were also generated. HIV-$1_{T66I/Q146P}$ showed high-level resistance to EVG (119-fold reduced susceptibility) (Table 3). Combinations of S147G with T66I/Q146P or E92Q further enhanced resistance, 412- and 356-fold, respectively.

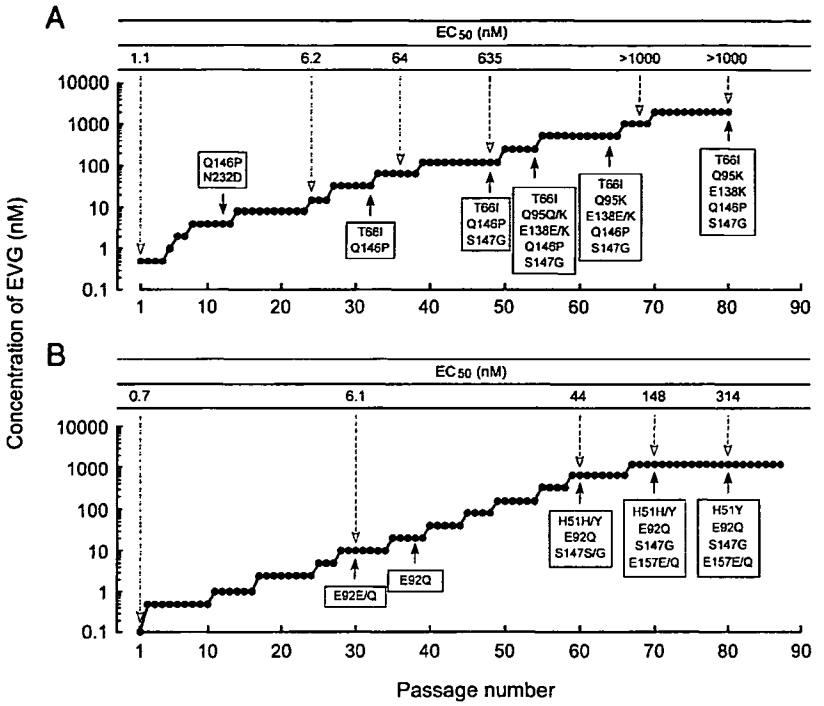

FIG. 3. Induction of EVG-resistant HIV-1. Data from MT-2 cells are shown. The initial concentrations of EVG were 0.5 nM (A) and 0.1 nM (B). Results are from two identical but independent experiments. At the indicated passage number (black arrowheads), proviral DNA extracted from infected MT-2 cells was sequenced. Amino acid substitutions are shown. The EC_{50} values of HIV-1 variants selected by EVG at the indicated passage number (white arrowheads) were determined using MAGI assay (A) or the production of p24 in MT-2 cells (B).

The triple mutant HIV-$1_{H51Y/E92Q/S147G}$ showed high-level resistance to EVG (700-fold reduced susceptibility). Interestingly, the addition of the secondary mutation H51Y, which on its own reduced EVG susceptibility only 3.6-fold, substantially enhanced resistance relative to that observed for the double mutant HIV-$1_{E92Q/S147G}$. HIV-$1_{T66I/Q95K/Q146P/S147G}$, HIV-$1_{T66I/Q95K/E138K/Q146P/S147G}$, and HIV-$1_{H51Y/E92Q/S147G/E157Q}$ mutants all showed high-level resistance to EVG, with EC_{50} values greater than 1,000 nM in all cases. These results indicate that the T66I and E92Q mutations provided the highest change (*n*-fold) in EVG susceptibility as individual resistance mutations and that the additional substitutions identified further enhance the level of resistance to EVG when combined with these primary mutations.

(ii) L-870,810-selected mutations. Infectious HIV-1 clones containing mutations (V72I, F121Y, T125K, and V151I) previously shown to be associated with resistance to L-870,810 (23) and two mutations, L74M and G163R, observed in our selection using L-870,810 (data not shown) were generated. Among these variants, HIV-1_{F121Y} and HIV-1_{V151I} demonstrated reduced susceptibility to both L-870,810 and EVG (Table 3). V151I has been observed in some HIV-1 clinical isolates and may be an IN polymorphism (34). Moreover, the effect of V151I on susceptibility to L-870,810 has been controversial (23, 29). This discrepancy might arise from the viral strain or plasmid backbone used, so further experiments to clarify the effect of V151I on IN inhibitor susceptibility are needed. HIV-$1_{F121Y/T125K}$ showed significant resistance to both L-870,810 and EVG (68-fold and 177-fold reduced susceptibility, respectively). HIV-$1_{V72I/F121Y/T125K/V151I}$ showed high-level resistance to both IN inhibitors (EC_{50} greater than 1,000 nM).

(iii) DKA IN inhibitor-selected mutations. Highlighting the potential for related mechanisms of IN inhibitor resistance and cross-resistance, the T66I mutation has also been observed to be selected by DKA IN inhibitors such as L-708,906 and S-1360. Additional mutations, L74M and S153Y, in combination with T66I were also observed to be selected by these DKA IN inhibitors (16, 17). L74M also emerged during L-870,810 selection in our studies (data not shown) but conferred no change in susceptibility to L-870,810 when present alone and only low-level resistance (3.0-fold) to EVG (Table 3). The combination of T66I and L74M conferred slightly higher resistance to EVG (45-fold) than did T66I alone but only moderate resistance to L-870,810 (7.1-fold). Another IN mutant, HIV-$1_{T66I/S153Y}$, observed in L-708,906 selection experiments (24) showed high-level resistance to EVG (260-fold) but low-level resistance to L-870,810 (5.0-fold). These results suggest that the mechanism of EVG resistance may have some similarities to that of DKA IN inhibitors.

Taken together, these results suggest that a variety of IN mutations may be selected by EVG and other IN inhibitors. Most of the IN inhibitor resistance mutations are observed to cluster in the CCD of IN. The resulting mutations and their combinations have the capacity to confer various levels of resistance and potential cross-resistance to EVG and other IN inhibitors. Given their location in the CCD, many of these mutations may act via a common mechanism. The observed development of IN inhibitor resistance mutations resembles

TABLE 3. Susceptibilities of HIV-1 IN recombinant molecular clones[a]

Molecular clone(s)	Mean EC_{50} (nM) ± SD (fold resistance compared to wild type)				
	AZT	EVG	L-870,810	S-1360	L-731,988
$HIV\text{-}1_{WT}$	32	1.1	5.8	1,239	736
EVG mutation (expt 1)[b]					
T66I[c]	43 ± 11 (1.3)	41 ± 14 (37)	4.7 ± 2.9 (0.8)	6,403 ± 2,349 (5.2)	7,234 ± 1,210 (9.8)
Q95K	34 ± 6 (1.1)	2.9 ± 0.4 (2.6)	18 ± 2 (3.1)	ND	ND
E138K	33 ± 8 (1.0)	1.1 ± 0.4 (1.0)	3.9 ± 0.4 (0.7)	ND	ND
Q146P	26 ± 2 (0.8)	12 ± 3 (11)	5.1 ± 0.4 (0.9)	ND	ND
S147G[d]	41 ± 5 (1.3)	12 ± 5 (11)	23 ± 6 (4.0)	ND	ND
T66I/Q146P	22 ± 2 (0.7)	131 ± 12 (119)	18 ± 5 (3.1)	ND	ND
T66I/Q146P/S147G	19 ± 5 (0.6)	453 ± 62 (412)	127 ± 37 (22)	ND	ND
T66I/Q95K/Q146P/S147G	31 ± 12 (1.0)	>1,000	303 ± 76 (52)	ND	ND
T66I/Q95K/E138K/Q146P/S147G	41 ± 7 (1.3)	>1,000	306 ± 76 (53)	>10,000	>50,000
EVG mutation (expt 2)[b]					
H51Y	34 ± 8 (1.1)	4.0 ± 0.6 (3.6)	3.3 ± 0.7 (0.6)	ND	ND
E92Q	32 ± 4 (1.0)	40 ± 12 (36)	63 ± 39 (11)	ND	ND
E157Q	34 ± 8 (1.1)	6.9 ± 1.4 (6.3)	52 ± 20 (9.0)	ND	ND
E92Q/S147G	39 ± 9 (1.2)	392 ± 133 (356)	587 ± 64 (101)	ND	ND
H51Y/E92Q/S147G	54 ± 6 (1.7)	769 ± 88 (699)	374 ± 100 (64)	>10,000	22,175 ± 1,299 (30)
H51Y/E92Q/S147G/E157Q	21 ± 2 (0.7)	>1,000	340 ± 26 (59)	>10,000	18,652 ± 4,575 (25)
L-870,810 mutation					
V72I	17 ± 1 (0.5)	4.3 ± 1.1 (3.9)	9.1 ± 2.5 (1.6)	ND	ND
L74M[c]	20 ± 3 (0.6)	3.3 ± 1.1 (3.0)	4.4 ± 1.7 (0.8)	1,500 ± 302 (1.2)	4,471 ± 942 (6.1)
F121Y	15 ± 1 (0.5)	28 ± 11 (25)	51 ± 23 (8.8)	ND	ND
T125K	17 ± 3 (0.5)	2.3 ± 1.1 (2.1)	9.9 ± 3.7 (1.7)	ND	ND
V151I	21 ± 4 (0.7)	11 ± 3 (10)	104 ± 29 (18)	ND	ND
G163R	22 ± 7 (0.7)	0.8 ± 0.2 (0.7)	6.5 ± 2.6 (1.1)	ND	ND
F121Y/G163R	36 ± 5 (1.1)	60 ± 20 (55)	219 ± 20 (38)	ND	ND
F121Y/T125K	38 ± 12 (1.2)	195 ± 73 (177)	393 ± 82 (68)	ND	ND
V72I/F121Y/T125K	33 ± 7 (1.0)	143 ± 25 (130)	886 ± 79 (153)	ND	ND
V72I/F121Y/T125K/V151I	64 ± 9 (2.0)	>1,000	>1,000	>10,000	>50,000
DKA mutation					
T66I/L74M	46 ± 11 (1.4)	49 ± 5 (45)	41 ± 10 (7.1)	>10,000	23,043 ± 4,886 (31)
T66I/S153Y	26 ± 8 (0.8)	285 ± 63 (259)	29 ± 9 (5.0)	>10,000	8,478 ± 1,267 (12)

[a] Antiviral activity was determined using the MAGI assay. Data shown are means and standard deviations obtained from at least three independent experiments, and resistance (*n*-fold) of the EC_{50} of the IN recombinant molecular clone compared to that of parental $HIV\text{-}1_{WT}$ is shown in parentheses. ND, not determined.
[b] EVG selection was performed in two independent experiments, and observed mutations are separately represented.
[c] Also observed in the DKA selected mutation.
[d] Observed in two independent EVG-selected experiments.

that seen for other antiretroviral drugs such as PIs; i.e., multiple mutations are introduced in a stepwise fashion and are required for high-level resistance to the selecting inhibitors (10, 50).

Strand transfer assay. To further characterize the effect of EVG-selected resistance mutations on IN function, the effect of mutations on the enzymatic activity of recombinant IN was evaluated in an in vitro strand transfer assay (Fig. 4). IN enzymes carrying the individual mutations H51Y, S147G, and E157Q had reduced strand transfer activity relative to that of the wild type (57%, 36%, and 79% of wild-type levels, respectively). Strand transfer activities of E92Q, E92Q/S147G, and H51Y/E92Q/S147G IN enzymes decreased with the accumulation of mutations from 57% to 29 and 22% of the wild type, respectively. However, the introduction of E157Q to H51Y/E92Q/S147Q partially restored strand transfer activity to 46% of wild-type activity, suggesting that E157Q may play a role in compensating for the loss of strand transfer activity resulting from the emergence of EVG resistance mutations.

The effect of EVG-selected mutations on the inhibition of strand transfer by EVG and L-870,810 was also determined (Fig. 4). Recombinant IN enzymes carrying the individual H51Y, S147G, and E157Q substitutions remained susceptible to both EVG and L-870,810 (0.7- to 2.1-fold reduced susceptibility). E92Q IN demonstrated only moderate resistance to both IN inhibitors in the strand transfer assay (4.3-fold reduced for both inhibitors). The combination of E92Q and S147G enhanced resistance to both EVG and L-870,810 (7.6- and 8.5-fold reduced susceptibility, respectively). However, unlike the IN recombinant viruses in the antiviral assay, neither the H51Y/E92Q/S147G nor the H51Y/E92Q/S147G/E157Q IN enzymes showed further enhancement of resistance in the strand transfer assay. This difference in results from the strand transfer assay versus those from the antiviral assay may reflect differences in the recombinant IN enzyme versus the viral IN enzyme in situ. Indeed, structure-activity relationship experiments described in a previous report (43) revealed that antiviral activity and in vitro enzyme inhibition were well correlated. Nevertheless, this biochemical analysis confirmed that the E92Q IN mutation confers significantly reduced suscepti-

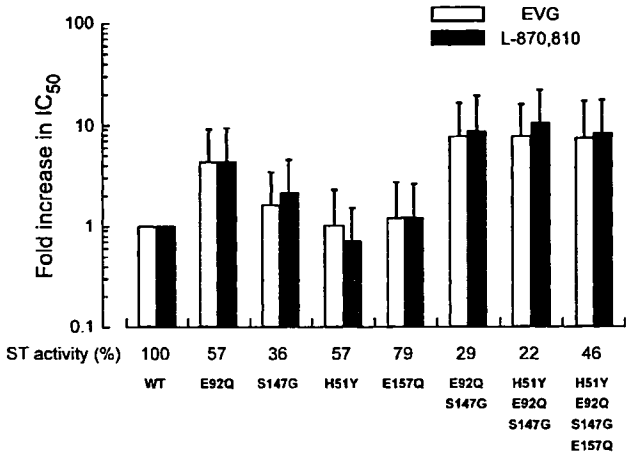

FIG. 4. Effect of EVG-selected mutations on IN strand transfer activity and on the inhibition of strand transfer by IN inhibitors. The strand transfer activities of recombinant IN enzymes carrying EVG-selected mutations were determined using an oligonucleotide-based strand transfer assay. Strand transfer (ST) activity of IN mutants was compared to that of the wild type (WT); results are shown as percentages of wild-type activity. The effect of IN inhibitors on strand transfer was also determined for wild-type and mutant IN enzymes; results are expressed as the increase (n-fold) in IC_{50} values of inhibitors relative to those of the wild type.

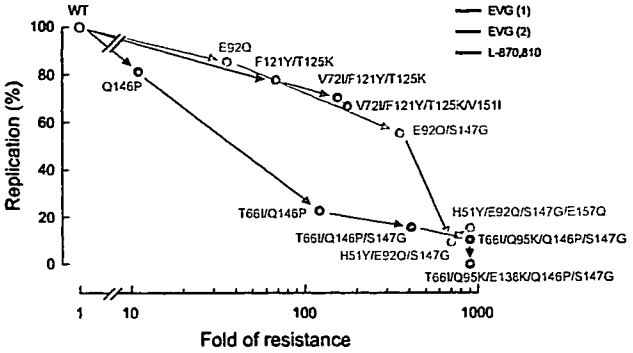

FIG. 5. Replication kinetics of EVG- and L-870,810-resistant viral variants. The replication kinetics of wild-type and IN inhibitor-resistant viral variants were determined by p24 ELISA. The relationship of replication capacity and change (n-fold) in susceptibility (shown in Table 3) is depicted. Variants are plotted according to the observed order of their emergence during selection experiments in vitro. Replication kinetics of EVG-selected mutants derived from the two independent selection experiments (shown in Fig. 3) are plotted in different colors. WT, wild type.

bility to EVG at the level of inhibition of strand transfer, consistent with its identification as a primary EVG resistance mutation in the virological analyses.

Replication kinetics of IN inhibitor-resistant variants. The effects of IN mutations on the replication kinetics of HIV-1 variants were assessed by comparing their levels of p24 production in culture supernatants to that of wild-type virus (Fig. 5). At day 5 postinfection, levels of p24 production by the HIV-1_{E92Q} and HIV-1_{Q146P} variants were 86% and 82% of HIV-1_{WT} levels, respectively. These variants showed high-level (36-fold) or moderate (11-fold) resistance to EVG (Table 3), whereas the replication levels of both were similar to those of the wild type. However, the introduction of additional EVG resistance mutations further decreased p24 production, which is indicative of a decline in the levels of viral replication. In particular, HIV-$1_{T66I/Q146P/S147G}$, HIV-$1_{T66I/Q95K/Q146P/S147G}$, HIV-$1_{T66I/Q95K/E138K/Q146P/S147G}$, HIV-$1_{H51Y/E92Q/S147G}$, and HIV-$1_{H51Y/E92Q/S147G/E157Q}$ all showed significantly reduced levels of p24 production (less than 20% of wild-type levels by day 5 in all cases). Thus, there was an inverse correlation between the levels of EVG resistance and the viral replication capacity; that is, as resistance to EVG increased, viral replication decreased. Interestingly, viral variants carrying L-870,810-selected mutations had more moderate reductions in replication capacity, even in the case of the HIV-$1_{V72I/F121Y/T125K/V151I}$ variant that had high-level resistance to both L-870,810 and EVG (68% of wild-type levels). These results indicate that mutations associated with resistance to IN inhibitors can have various effects on viral replication capacity. The reduced replication capacity of EVG-resistant variants was not rescued in the presence of the inhibitor (data not shown), as was observed previously for NFV-resistant variants in the presence of NFV (35). Thus, the reduced replication capacity of IN inhibitor-resistant variants may present a barrier to their emergence in vivo.

Antiviral effect of IN inhibitors on retroviruses. The antiviral activity of EVG against other retroviruses, including MLV and SIV, was assessed. EVG and L-870,810 inhibited the integration of the HIV-based vector used as a positive control for the luciferase assay (EC_{50} values of 0.8 and 5.0 nM, respectively), as observed in the MAGI assay with HIV-1_{IIIB} (Fig. 6). EVG and L-870,810 suppressed the replication of MLV infection (EC_{50} values of 5.8 and 22 nM, respectively) as well as that of the primate retrovirus SIV (0.5 and 3.2 nM, respectively), indicating that IN inhibitors have antiviral activity against a broad range of retroviruses.

DISCUSSION

The data described here show that EVG inhibits HIV replication by specifically blocking the strand transfer reaction mediated by IN, as demonstrated by the intracellular accumulation of 2-LTR DNA products, a signature of nonproductive integration. Furthermore, EVG directly blocked the production of strand transfer products in an in vitro strand transfer assay. Confirming that EVG is a bona fide IN inhibitor, we selected EVG-resistant viral variants in vitro and demonstrated that the resulting viral variants had acquired multiple mutations in the IN coding region and had simultaneously acquired reduced phenotypic susceptibility to EVG. HIV-1 molecular clones carrying the EVG-selected IN mutations had an EVG-resistant phenotype and in many cases also had reduced susceptibility to another IN inhibitor, L-870,810. These data provide formal proof that the observed IN mutations are indeed EVG resistance mutations and that EVG is an IN inhibitor.

Among the IN mutations observed to be selected by EVG, two mutations, T66I and E92Q, appeared to provide the major contribution to EVG resistance. Both of these individual mutations resulted in >30-fold reduced susceptibility to EVG. The T66I mutation conferred cross-resistance to S-1360 and

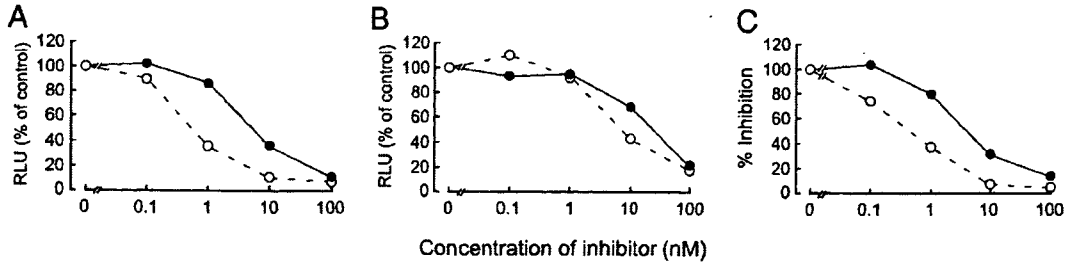

FIG. 6. Effect of IN inhibitors on retroviruses. Antiviral activities of EVG (open circles with dashed lines) and L-870,810 (closed circles with solid lines) against HIV-based (A) or MLV-based (B) vectors harboring the luciferase gene were determined by measuring luciferase activity at 48 h posttransduction. Results are expressed as percentages of relative luciferase units (RLU) compared to those of the no-inhibitor control. (C) Anti-SIV activity was determined using the MAGI assay. These results shown are one representative assay from three independent experiments.

L-731,988 (Table 3) and was also previously observed in an independent EVG selection by Jones et al. (26). The E92Q mutation, when introduced into a recombinant IN enzyme, also reduced the susceptibility of the resulting mutant IN enzyme to EVG, as measured by the reduced EVG inhibition of the in vitro strand transfer assay (Fig. 4). The other IN mutations identified, including H51Y, Q95K, E138K, Q146P, S147G, and E157Q, individually resulted in lower changes (*n*-fold) in EVG susceptibility (1.0- to 11.0-fold) but, when added to either the T66I or the E92Q mutation, further increased resistance to EVG to various degrees relative to either mutation alone. Interestingly, the accumulation of these EVG-selected IN mutations resulted in a significant attenuation of viral replication kinetics. Thus, the emergence of resistance to IN inhibitors may be associated with reductions in viral fitness, which may provide a barrier to the emergence of these mutations in vivo or be associated with lower viral loads if they do emerge.

Of the three HIV enzymes PR, RT, and IN, the structure and mechanism of IN are the least well understood, and despite extensive efforts, the structure of the complete IN enzyme remains to be determined. Only partial two-domain crystal structures of the IN apoenzyme are available, and no structure showing full-length IN bound to its viral cDNA substrate has been published. During integration in vivo, IN functions in the preintegration complex, which also includes RT and the viral DNA (2, 3). Some limited evidence suggests that RT interacts with the active site of IN (39). IN has also been proposed to function with several cellular factors including IN interactor 1 (Ini1) (27) and lens-epithelium-derived growth factor (LEDGF/p75) (7). In the context of these associated cellular factors, IN may retain a different conformation compared to that of the recombinant enzyme alone. This may be one of the reasons that only moderate EVG resistance was observed in the oligonucleotide-based strand transfer assay compared to a cell-based antiviral assay.

Alignment of several IN CCD structures deposited in the Protein Data Bank indicates that there are two regions with poorly defined or disordered structures, including residues 47 to 56 and 140 to 152 (Fig. 7; see Fig. S1 in the supplemental material). Of these two disordered regions, residues 140 to 152 have been implicated as a flexible loop involved in viral cDNA binding (20, 21, 53). Although the precise structural details are unknown, the flexible loop has been proposed to adopt different conformations in the presence or absence of the viral cDNA (12). Notably, several of the EVG-selected mutations that we observed are located on or adjacent to this proposed flexible loop, including E138K, Q146P, and S147G. The flexible loop is important for the catalytic activity of IN (21, 32), and as shown in Fig. 4, the introduction of mutations in these residues, especially S147G, drastically reduced the catalytic activity of IN. Previously published data also demonstrated that another mutation at codon 147 (S147I) resulted in HIV-1 that was highly replication defective, including effects on viral DNA synthesis (47). Indeed, S147 is highly conserved among various retroviruses (see Fig. S2 in the supplemental material), highlighting the importance of the loop for IN function. It is possible that IN inhibitor resistance mutants may have additional pleiotropic effects on processes in viral replication other

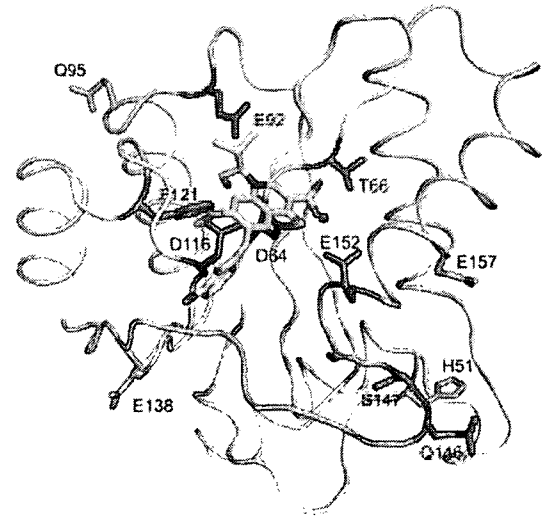

FIG. 7. Location of IN mutations associated with resistance to EVG. EVG in complex with the HIV-1 IN CCD is shown along with the catalytic triad residues (D64, D116, and E152) (green) and a magnesium ion (magenta). Amino acid residues conferring resistance to EVG as primary mutations (T66, E92, F121, Q146, and S147) or as secondary mutations (H51, Q95, E138, and E157) are shown in red and cyan, respectively. The flexible loop (residues 140 to 152) is shown in pink.

than integration; in particular, RT and IN were previously suggested to interact functionally (25).

Recently, an in silico docking simulation of HIV IN with several IN inhibitors including EVG was reported (44). Notably, that author showed that in the best-fit model for EVG docked to IN, the isobutyl substituent on the quionolone moiety of EVG orients directly towards IN residue E92. Interestingly, the hydroxyl component of the isobutyl on the quinolone replaces a water molecule that is coordinated by residue E92 between the two catalytic residues D64 and E152. This docking structure may provide insight into the mechanism of IN inhibition by EVG and provides a starting point for understanding the mechanism of EVG resistance mediated by the E92Q substitution. However, it is uncertain whether this docking simulation represents the precise binding mode of EVG with IN in vivo. Therefore, to accurately assess the binding mode of IN inhibitors with IN, available structural data need to be supplemented by a variety of other approaches. In this study, a virological approach and an enzymatic approach were integrated to characterize the mechanism of action, antiviral activity, and resistance profile of EVG in vitro.

As shown in Fig. 7, primary EVG resistance mutations are located around the catalytic triad of the CCD of IN and are surrounded by the secondary mutations. Among the residues affected by primary mutations, E92 and F121 are located close to EVG on the model and might interact with the IN inhibitor. However, the mechanism by which these mutations interact with the IN inhibitor or with the viral cDNA to mediate resistance is currently unclear. Recently, clinical isolate data from patients experiencing virologic failure in ongoing phase III studies of another IN inhibitor, raltegravir, were reported; E92Q was among the mutations noted to develop in these raltegravir failure patients, usually in combination with another IN mutation, N155H (11, 48). These preliminary clinical data and the data presented here with L-870,810, indicate that the E92Q mutation may be able to mediate resistance and potential cross-resistance to multiple IN inhibitors including EVG and raltegravir. Consistent with the data described here, site-directed mutant HIV carrying the E92Q mutation has been confirmed to show resistance to EVG and to have low-level (approximately sixfold) reduced susceptibility to raltegravir (26).

Several of the IN residues affected by primary mutations observed in EVG-selected variants including T66, E92, and S147 are absolutely conserved among the retroviruses tested (HIV-1, HIV-2, SIV, and MLV) and in retroviruses from multiple mammalian species (see Fig. S2 in the supplemental material). The significant conservation of mammalian retroviral IN CCDs at both the level of sequence homology and structure of the active site was demonstrated by the ability of EVG to inhibit HIV, SIV, and MLV IN activity. This suggests that EVG, and probably other IN inhibitors, binds to a conformationally conserved region of all retroviral INs; the binding of EVG and other IN inhibitors to IN is also likely to involve the catalytic magnesium ion. Taken together, these results suggest that several distinct mechanisms may contribute to IN inhibitor resistance, including conformational changes in the structure of IN that affect the binding of the IN inhibitor, charge effects, steric hindrance, loss of stabilizing binding interactions, or, possibly, alterations in magnesium binding.

A similar reduction in viral replication capacity as a result of drug resistance mutations was previously reported for NRTI resistance mutations (K65R, L74V, and M184V) (45, 55) and for PI resistance mutations (D30N) (49). Mutations that act to compensate for some of the loss of viral replication resulting from drug resistance, for example, GAG processing mutants, have also been described (18, 36, 52). At least one of the EVG secondary mutations, E157Q, may have an analogous role, as it partially restored strand transfer activity that was attenuated by other EVG-selected mutations and also further enhanced resistance to EVG (Fig. 4). Some secondary IN mutations might act to compensate for the altered conformation of IN resulting from the structural effects of primary resistance mutations. The E138K mutation may be such an example, as on its own, it showed no effect on susceptibility to either EVG or L-870,810. The clinical implications of the reduction in fitness resulting from the selection of EVG-resistant mutations are not yet understood.

In conclusion, EVG is a potent inhibitor of the HIV IN enzyme that acts by blocking the strand transfer reaction and is effective not only against HIV but also against other retroviruses. Moreover, the emergence of viral variants that were highly resistant to EVG was associated with significant reductions in viral replication in vitro. These results indicate that EVG should be highly effective for the treatment of HIV-1-infected patients, including those who have had virologic failure of their highly active antiretroviral therapy due to the emergence of HIV-1 drug resistance to approved antiretroviral drugs.

ACKNOWLEDGMENTS

We thank Shinjiro Hino for technical advice and Mieko Ikeuchi for technical assistance. We appreciate Damian McColl for critically reading and commenting on the manuscript.

This work was supported in part by a grant for the Promotion of AIDS Research from the Ministry of Health and Welfare of Japan (E.K. and M.M.), a grant for Research for Health Science Focusing on Drug Innovation from the Japan Health Science Foundation (E.K. and M.M.), and a grant from the Ministry of Education, Culture, Sports, Science, and Technology of Japan (E.K.). K.S. is supported by the 21st Century COE Program of the Ministry of Education, Culture, Sports, Science, and Technology.

REFERENCES

1. **Asante-Appiah, E., and A. M. Skalka.** 1997. Molecular mechanisms in retrovirus DNA integration. Antivir. Res. 36:139–156.
2. **Brown, P. O., B. Bowerman, H. E. Varmus, and J. M. Bishop.** 1987. Correct integration of retroviral DNA in vitro. Cell 49:347–356.
3. **Bukrinsky, M. I., N. Sharova, T. L. McDonald, T. Pushkarskaya, W. G. Tarpley, and M. Stevenson.** 1993. Association of integrase, matrix, and reverse transcriptase antigens of human immunodeficiency virus type 1 with viral nucleic acids following acute infection. Proc. Natl. Acad. Sci. USA 90:6125–6129.
4. **Butler, S. L., M. S. Hansen, and F. D. Bushman.** 2001. A quantitative assay for HIV DNA integration in vivo. Nat. Med. 7:631–634.
5. **Chackerian, B., E. M. Long, P. A. Luciw, and J. Overbaugh.** 1997. Human immunodeficiency virus type 1 coreceptors participate in postentry stages in the virus replication cycle and function in simian immunodeficiency virus infection. J. Virol. 71:3932–3939.
6. **Chakrabarti, L. A., K. J. Metzner, T. Ivanovic, H. Cheng, J. Louis-Virelizier, R. I. Connor, and C. Cheng-Mayer.** 2003. A truncated form of Nef selected during pathogenic reversion of simian immunodeficiency virus SIVmac239Δnef increases viral replication. J. Virol. 77:1245–1256.
7. **Cherepanov, P., G. Maertens, P. Proost, B. Devreese, J. Van Beeumen, Y. Engelborghs, E. De Clercq, and Z. Debyser.** 2003. HIV-1 integrase forms stable tetramers and associates with LEDGF/p75 protein in human cells. J. Biol. Chem. 278:372–381.
8. **Chow, S. A.** 1997. In vitro assays for activities of retroviral integrase. Methods 12:306–317.

9. **Clavel, F., and A. J. Hance.** 2004. HIV drug resistance. N. Engl. J. Med. 350:1023–1035.
10. **Condra, J. H., W. A. Schleif, O. M. Blahy, L. J. Gabryelski, D. J. Graham, J. C. Quintero, A. Rhodes, H. L. Robbins, E. Roth, M. Shivaprakash, D. Titus, T. Yang, H. Tepplert, K. E. Squires, P. J. Deutsch, and E. A. Emini.** 1995. In vivo emergence of HIV-1 variants resistant to multiple protease inhibitors. Nature 374:569–571.
11. **Cooper, D., J. Gatell, J. Rockstroh, C. Katlama, P. Yeni, A. Lazzarin, J. Chen, R. Isaacs, H. Teppler, and B. Nguyen for the BENCHMRK-1 Study Group.** 2007. Abstr. 14th Conf. Retrovir. Opportun. Infect., abstr. 105aLB.
12. **De Luca, L., G. Vistoli, A. Pedretti, M. L. Barreca, and A. Chimirri.** 2005. Molecular dynamics studies of the full-length integrase-DNA complex. Biochem. Biophys. Res. Commun. 336:1010–1016.
13. **Dyda, F., A. B. Hickman, T. M. Jenkins, A. Engelman, R. Craigie, and D. R. Davies.** 1994. Crystal structure of the catalytic domain of HIV-1 integrase: similarity to other polynucleotidyl transferases. Science 266:1981–1986.
14. **Engelman, A., K. Mizuuchi, and R. Craigie.** 1991. HIV-1 DNA integration: mechanism of viral DNA cleavage and DNA strand transfer. Cell 67:1211–1221.
15. **Fan, J., E. Kodama, Y. Koh, M. Nakao, and M. Matsuoka.** 2005. Halogenated thymidine analogues restore the expression of silenced genes without demethylation. Cancer Res. 65:6927–6933.
16. **Fikkert, V., A. Hombrouck, B. Van Remoortel, M. De Maeyer, C. Pannecouque, E. De Clercq, Z. Debyser, and M. Witvrouw.** 2004. Multiple mutations in human immunodeficiency virus-1 integrase confer resistance to the clinical trial drug S-1360. AIDS 18:2019–2028.
17. **Fikkert, V., B. Van Maele, J. Vercammen, A. Hantson, B. Van Remoortel, M. Michiels, C. Gurnari, C. Pannecouque, M. De Maeyer, Y. Engelborghs, E. De Clercq, Z. Debyser, and M. Witvrouw.** 2003. Development of resistance against diketo derivatives of human immunodeficiency virus type 1 by progressive accumulation of integrase mutations. J. Virol. 77:11459–11470.
18. **Gatanaga, H., Y. Suzuki, H. Tsang, K. Yoshimura, M. F. Kavlick, K. Nagashima, R. J. Gorelick, S. Mardy, C. Tang, M. F. Summers, and H. Mitsuya.** 2002. Amino acid substitutions in Gag protein at non-cleavage sites are indispensable for the development of a high multitude of HIV-1 resistance against protease inhibitors. J. Biol. Chem. 277:5952–5961.
19. **Goldgur, Y., R. Craigie, G. H. Cohen, T. Fujiwara, T. Yoshinaga, T. Fujishita, H. Sugimoto, T. Endo, H. Murai, and D. R. Davies.** 1999. Structure of the HIV-1 integrase catalytic domain complexed with an inhibitor: a platform for antiviral drug design. Proc. Natl. Acad. Sci. USA 96:13040–13043.
20. **Goldgur, Y., F. Dyda, A. B. Hickman, T. M. Jenkins, R. Craigie, and D. R. Davies.** 1998. Three new structures of the core domain of HIV-1 integrase: an active site that binds magnesium. Proc. Natl. Acad. Sci. USA 95:9150–9154.
21. **Greenwald, J., V. Le, S. L. Butler, F. D. Bushman, and S. Choe.** 1999. The mobility of an HIV-1 integrase active site loop is correlated with catalytic activity. Biochemistry 38:8892–8898.
22. **Grinsztejn, B., B. Y. Nguyen, C. Katlama, J. M. Gatell, A. Lazzarin, D. Vittecoq, C. J. Gonzalez, J. Chen, C. M. Harvey, and R. D. Isaacs.** 2007. Safety and efficacy of the HIV-1 integrase inhibitor raltegravir (MK-0518) in treatment-experienced patients with multidrug-resistant virus: a phase II randomised controlled trial. Lancet 369:1261–1269.
23. **Hazuda, D. J., N. J. Anthony, R. P. Gomez, S. M. Jolly, J. S. Wai, L. Zhuang, T. E. Fisher, M. Embrey, J. P. Guare, Jr., M. S. Egbertson, J. P. Vacca, J. R. Huff, P. J. Felock, M. V. Witmer, K. A. Stillmock, R. Danovich, J. Grobler, M. D. Miller, A. S. Espeseth, L. Jin, I. W. Chen, J. H. Lin, K. Kassahun, J. D. Ellis, B. K. Wong, W. Xu, P. G. Pearson, W. A. Schleif, R. Cortese, E. Emini, V. Summa, M. K. Holloway, and S. D. Young.** 2004. A naphthyridine carboxamide provides evidence for discordant resistance between mechanistically identical inhibitors of HIV-1 integrase. Proc. Natl. Acad. Sci. USA 101:11233–11238.
24. **Hazuda, D. J., P. Felock, M. Witmer, A. Wolfe, K. Stillmock, J. A. Grobler, A. Espeseth, L. Gabryelski, W. Schleif, C. Blau, and M. D. Miller.** 2000. Inhibitors of strand transfer that prevent integration and inhibit HIV-1 replication in cells. Science 287:646–650.
25. **Hehl, E. A., P. Joshi, G. V. Kalpana, and V. R. Prasad.** 2004. Interaction between human immunodeficiency virus type 1 reverse transcriptase and integrase proteins. J. Virol. 78:5056–5067.
26. **Jones, G., R. Ledford, F. Yu, M. Miller, M. Tsiang, and D. McColl.** 2007. Abstr. 14th Conf. Retrovir. Opportun. Infect., abstr. 627.
27. **Kalpana, G. V., S. Marmon, W. Wang, G. R. Crabtree, and S. P. Goff.** 1994. Binding and stimulation of HIV-1 integrase by a human homolog of yeast transcription factor SNF5. Science 266:2002–2006.
28. **Kaufmann, G. R., and D. A. Cooper.** 2000. Antiretroviral therapy of HIV-1 infection: established treatment strategies and new therapeutic options. Curr. Opin. Microbiol. 3:508–514.
29. **Kehlenbeck, S., U. Betz, A. Birkmann, B. Fast, A. H. Goller, K. Henninger, T. Lowinger, D. Marrero, A. Paessens, D. Paulsen, V. Pevzner, R. Schohe-Loop, H. Tsujishita, R. Welker, J. Kreuter, H. Rubsamen-Waigmann, and F. Dittmer.** 2006. Dihydroxythiophenes are novel potent inhibitors of human immunodeficiency virus integrase with a diketo acid-like pharmacophore. J. Virol. 80:6883–6894.
30. **Kodama, E. I., S. Kohgo, K. Kitano, H. Machida, H. Gatanaga, S. Shigeta, M. Matsuoka, H. Ohrui, and H. Mitsuya.** 2001. 4′-Ethynyl nucleoside analogs: potent inhibitors of multidrug-resistant human immunodeficiency virus variants in vitro. Antimicrob. Agents Chemother. 45:1539–1546.
31. **LaFemina, R. L., C. L. Schneider, H. L. Robbins, P. L. Callahan, K. LeGrow, E. Roth, W. A. Schleif, and E. A. Emini.** 1992. Requirement of active human immunodeficiency virus type 1 integrase enzyme for productive infection of human T-lymphoid cells. J. Virol. 66:7414–7419.
32. **Lee, M. C., J. Deng, J. M. Briggs, and Y. Duan.** 2005. Large-scale conformational dynamics of the HIV-1 integrase core domain and its catalytic loop mutants. Biophys. J. 88:3133–3146.
33. **Little, S., G. Drusano, R. Schooley, D. Haas, P. Kumar, S. Hammer, D. McMahon, K. Squires, R. Asfour, D. Richman, J. Chen, A. Saah, R. Leavitt, D. Hazuda, B. Y. Nguyen, and the Protocol 004 Study Team.** 2005. Abstr. 12th Conf. Retrovir. Opportun. Infect., abstr. 161.
34. **Los Alamos National Laboratory Theoretical Biology and Biophysics Group T-10.** 2001. HIV sequence compendium, 2001. Theoretical Biology and Biophysics Group, Los Alamos National Laboratory, Los Alamos, NM.
35. **Matsuoka-Aizawa, S., H. Sato, A. Hachiya, K. Tsuchiya, Y. Takebe, H. Gatanaga, S. Kimura, and S. Oka.** 2003. Isolation and molecular characterization of a nelfinavir (NFV)-resistant human immunodeficiency virus type 1 that exhibits NFV-dependent enhancement of replication. J. Virol. 77:318–327.
36. **Myint, L., M. Matsuda, Z. Matsuda, Y. Yokomaku, T. Chiba, A. Okano, K. Yamada, and W. Sugiura.** 2004. Gag non-cleavage site mutations contribute to full recovery of viral fitness in protease inhibitor-resistant human immunodeficiency virus type 1. Antimicrob. Agents Chemother. 48:444–452.
37. **Nameki, D., E. Kodama, M. Ikeuchi, N. Mabuchi, A. Otaka, H. Tamamura, M. Ohno, N. Fujii, and M. Matsuoka.** 2005. Mutations conferring resistance to human immunodeficiency virus type 1 fusion inhibitors are restricted by gp41 and Rev-responsive element functions. J. Virol. 79:764–770.
38. **Neuveut, C., and K. T. Jeang.** 1996. Recombinant human immunodeficiency virus type 1 genomes with *tat* unconstrained by overlapping reading frames reveal residues in Tat important for replication in tissue culture. J. Virol. 70:5572–5581.
39. **Oz Gleenberg, I., O. Avidan, Y. Goldgur, A. Herschhorn, and A. Hizi.** 2005. Peptides derived from the reverse transcriptase of human immunodeficiency virus type 1 as novel inhibitors of the viral integrase. J. Biol. Chem. 280:21987–21996.
40. **Palella, F. J., Jr., K. M. Delaney, A. C. Moorman, M. O. Loveless, J. Fuhrer, G. A. Satten, D. J. Aschman, S. D. Holmberg, et al.** 1998. Declining morbidity and mortality among patients with advanced human immunodeficiency virus infection. N. Engl. J. Med. 338:853–860.
41. **Pommier, Y., A. A. Johnson, and C. Marchand.** 2005. Integrase inhibitors to treat HIV/AIDS. Nat. Rev. Drug Discov. 4:236–248.
42. **Reinke, R., D. J. Lee, and W. E. Robinson, Jr.** 2002. Inhibition of human immunodeficiency virus type 1 isolates by the integrase inhibitor L-731,988, a diketo acid. Antimicrob. Agents Chemother. 46:3301–3303.
43. **Sato, M., T. Motomura, H. Aramaki, T. Matsuda, M. Yamashita, Y. Ito, H. Kawakami, Y. Matsuzaki, W. Watanabe, K. Yamataka, S. Ikeda, E. Kodama, M. Matsuoka, and H. Shinkai.** 2006. Novel HIV-1 integrase inhibitors derived from quinolone antibiotics. J. Med. Chem. 49:1506–1508.
44. **Savarino, A.** 2007. In-silico docking of HIV-1 integrase inhibitors reveals a novel drug type acting on an enzyme/DNA reaction intermediate. Retrovirology 4:21.
45. **Sharma, P. L., and C. S. Crumpacker.** 1997. Attenuated replication of human immunodeficiency virus type 1 with a didanosine-selected reverse transcriptase mutation. J. Virol. 71:8846–8851.
46. **Shibata, R., M. Kawamura, H. Sakai, M. Hayami, A. Ishimoto, and A. Adachi.** 1991. Generation of a chimeric human and simian immunodeficiency virus infectious to monkey peripheral blood mononuclear cells. J. Virol. 65:3514–3520.
47. **Shin, C. G., B. Taddeo, W. A. Haseltine, and C. M. Farnet.** 1994. Genetic analysis of the human immunodeficiency virus type 1 integrase protein. J. Virol. 68:1633–1642.
48. **Steigbigel, R., P. Kumar, J. Eron, M. Schechter, M. Markowitz, M. Loufty, J. Zhao, R. Isaacs, B. Nguyen, H. Teppler, and the BENCHMRK-2 Study Group.** 2007. Abstr. 14th Conf. Retrovir. Opportun. Infect., abstr. 105bLB.
49. **Sugiura, W., Z. Matsuda, Y. Yokomaku, K. Hertogs, B. Larder, T. Oishi, A. Okano, T. Shiino, M. Tatsumi, M. Matsuda, H. Abumi, N. Takata, S. Shirahata, K. Yamada, H. Yoshikura, and Y. Nagai.** 2002. Interference between D30N and L90M in selection and development of protease inhibitor-resistant human immunodeficiency virus type 1. Antimicrob. Agents Chemother. 46:708–715.
50. **Tisdale, M., R. E. Myers, B. Maschera, N. R. Parry, N. M. Oliver, and E. D. Blair.** 1995. Cross-resistance analysis of human immunodeficiency virus type 1 variants individually selected for resistance to five different protease inhibitors. Antimicrob. Agents Chemother. 39:1704–1710.
51. **Toossi, Z., H. Mayanja-Kizza, J. Baseke, P. Peters, M. Wu, A. Abraha, H. Aung, A. Okwera, C. Hirsch, and E. Arts.** 2005. Inhibition of human immu-

nodeficiency virus-1 (HIV-1) by beta-chemokine analogues in mononuclear cells from HIV-1-infected patients with active tuberculosis. Clin. Exp. Immunol. 142:327–332.
52. **Verheyen, J., E. Litau, T. Sing, M. Daumer, M. Balduin, M. Oette, G. Fatkenheuer, J. K. Rockstroh, U. Schuldenzucker, D. Hoffmann, H. Pfister, and R. Kaiser.** 2006. Compensatory mutations at the HIV cleavage sites p7/p1 and p1/p6-gag in therapy-naive and therapy-experienced patients. Antivir. Ther. 11:879–887.
53. **Wang, J. Y., H. Ling, W. Yang, and R. Craigie.** 2001. Structure of a two-domain fragment of HIV-1 integrase: implications for domain organization in the intact protein. EMBO J. 20:7333–7343.
54. **Weiner, M. P., G. L. Costa, W. Schoettlin, J. Cline, E. Mathur, and J. C. Bauer.** 1994. Site-directed mutagenesis of double-stranded DNA by the polymerase chain reaction. Gene 151:119–123.
55. **White, K. L., N. A. Margot, T. Wrin, C. J. Petropoulos, M. D. Miller, and L. K. Naeger.** 2002. Molecular mechanisms of resistance to human immunodeficiency virus type 1 with reverse transcriptase mutations K65R and K65R+M184V and their effects on enzyme function and viral replication capacity. Antimicrob. Agents Chemother. 46:3437–3446.
56. **Zolopa, A., M. Mullen, D. Berger, P. Ruane, T. Hawkins, L. Zhong, S. Chuck, J. Enejosa, B. Kearney, and A. Cheng.** 2007. Abstr. 14th Confer. Retrovir. Opportun. Infect., abstr. 143LB.

JOURNAL OF VIROLOGY, Apr. 2007, p. 3757–3768 Vol. 81, No. 8
0022-538X/07/$08.00+0 doi:10.1128/JVI.01544-06

Impact of V2 Mutations on Escape from a Potent Neutralizing Anti-V3 Monoclonal Antibody during In Vitro Selection of a Primary Human Immunodeficiency Virus Type 1 Isolate[▽]

Junji Shibata,[1] Kazuhisa Yoshimura,[1] Akiko Honda,[1] Atsushi Koito,[1] Toshio Murakami,[2] and Shuzo Matsushita[1]*

Division of Clinical Retrovirology and Infectious Diseases, Center for AIDS Research, Kumamoto University, Kumamoto 860-0811,[1] and The Chemo-Sero-Therapeutic Research Institute, Kyokushi, Kikuchi, Kumamoto 869-1298,[2] Japan

Received 19 July 2006/Accepted 16 January 2007

KD-247, a humanized monoclonal antibody to an epitope of gp120-V3 tip, has potent cross-neutralizing activity against subtype B primary human immunodeficiency virus type 1 (HIV-1) isolates. To assess how KD-247 escape mutants can be generated, we induced escape variants by exposing bulked primary R5 virus, MOKW, to increasing concentrations of KD-247 in vitro. In the presence of relatively low concentrations of KD-247, viruses with two amino acid mutations (R166K/D167N) in V2 expanded, and under high KD-247 pressure, a V3 tip substitution (P313L) emerged in addition to the V2 mutations. However, a virus with a V2 175P mutation dominated during passaging in the absence of KD-247. Using domain swapping analysis, we demonstrated that the V2 mutations and the P313L mutation in V3 contribute to partial and complete resistance phenotypes against KD-247, respectively. To identify the V2 mutation responsible for the resistance to KD-247, we constructed pseudoviruses with single or double amino acid mutations in V2 and measured their sensitivity to neutralization. Interestingly, the neutralization phenotypes were switched, so that amino acid residue 175 (Pro or Leu) located in the center of V2 was exchanged, indicating that the amino acid at position 175 has a crucial role, dramatically changing the Env oligomeric state on the membrane surface and affecting the neutralization phenotype against not only anti-V3 antibody but also recombinant soluble CD4. These data suggested that HIV-1 can escape from anti-V3 antibody attack by changing the conformation of the functional envelope oligomer by acquiring mutations in the V2 region in environments with relatively low antibody concentrations.

The envelope protein (Env) of human immunodeficiency virus type 1 (HIV-1) presents on the virus surface as "spikes" composed of trimers comprising three gp120-gp41 complexes (6, 32, 33). Among the regions that induce the neutralization antibody (NAb) response, the third variable domain (V3 loop) of gp120 is considered one of the major targets of the host immune response (23, 69). It has been estimated that as much as half of the antibody response against HIV-1 Env in patient serum is directed against the V3 region (43). A recent crystallographic study revealed that the V3 loop contains features that are essential for coreceptor binding and that the extended nature and antibody accessibility of V3 are associated with its immunodominance (20).

HIV-1 primary isolates are relatively resistant to neutralization by NAbs and recombinant soluble CD4 (rsCD4) compared with variants selected for growth in permanent cell lines (42, 52, 55). Studies addressing differences between neutralization-sensitive and -resistant variants have revealed the involvement of several mechanisms that underlie the neutralization resistance of primary isolates, including the occlusion of epitopes within the oligomer, extensive glycosylation, and extension of variable loops from the surface of the complex, as well as steric and conformational blocking of receptor binding sites (7, 12, 32, 38, 49, 50, 54, 62). The structural features of gp120 tolerate a vast array of mutations that permit the selection of neutralization escape variants, as has been previously demonstrated in culture assays, animal models, and infected individuals (24).

Although there are ample data showing that NAbs can protect against HIV-1 infection in vitro and in animal models in vivo, activity in infected humans remains controversial (3, 4, 9, 14, 22, 40, 48, 58). Studies addressing NAbs in primary infections have suggested that most recently infected individuals mount a vigorous antibody response against autologous viruses. However, the rapid evolution of HIV in the presence of NAbs results in the emergence of escape mutants. As a consequence, at any time during an early stage of the HIV disease, NAbs are more likely to recognize earlier autologous viruses than contemporaneous ones. Despite evidence of phenotypic resistance, the genetic basis of the mechanism allowing primary viruses to escape from NAbs is poorly understood. Wei et al. found that glycosylation in the envelope plays an important role in allowing escape from neutralization (62). In contrast, in a recent study Frost et al. found that viral escape from NAbs is correlated with the rate of amino acid substitution rather than changes in glycosylation or insertions or deletions in the envelope (14). Because of the polyclonal nature of NAbs in patient sera, it is difficult to clarify the genetic mechanism responsible for neutralization escape.

* Corresponding author. Mailing address: Division of Clinical Retrovirology and Infectious Diseases, Center for AIDS Research, Kumamoto University, Kumamoto 860-0811, Japan. Phone: 81 96 373 6536. Fax: 81 96 373 6537. E-mail: shuzo@kaiju.medic.kumamoto-u.ac.jp.

▽ Published ahead of print on 24 January 2007.

Neutralization escape from anti-V3 monoclonal antibodies (MAbs) has been induced in T-cell-line-adapted viruses in several experiments and associated with amino acid substitution within the epitope in the V3 loop (8, 37, 65). However, Park et al. showed that human sera with neutralizing antibodies that contained polyclonal antibodies directed at the V3 region induced neutralization-resistant variants without V3 amino acid substitution (46). Neutralization studies using anti-V3 antibodies against primary isolates suggest that the neutralization resistance phenotype is associated with changes in the sequences outside V3, rather than variation within the V3 epitope (29, 62). However, the contribution of each change in the envelope to the emergence of escape mutants remains unclear because they are not selected under neutralizing MAb pressure.

Recently, we described a humanized MAb, KD-247, that displayed cross-neutralizing activity against HIV-1 clade B isolates (11). The epitope of KD-247 was mapped to six amino acids around the PGR core sequence at the tip of the V3 loop. The shortest reactive peptide recognized by KD-247 was determined to be IGPGR, which is shared by 49% of HIV-1 isolates in clade B (35). In addition, complete protection from challenge infection by a pathogenic strain of simian-human immunodeficiency virus 89.6 was observed when a high concentration of the antibody was used in an animal model (10). A molecularly cloned CCR5-tropic HIV-1 strain, JR-FL, which is relatively resistant to neutralization (15, 50), was exposed to KD-247 to obtain a neutralization escape mutant (67). Induction of the neutralization-resistant virus with a mutation in the V3 tip was observed in the presence of a high concentration of KD-247, and the escape variant was found to be more sensitive to CCR5 inhibitors and rsCD4 than the original strain (67).

The present study sought to understand how virus mutation impacts the activity of an anti-V3 MAb, KD-247. For this we subjected a primary R5 virus, MOKW, to selection pressure by KD-247. The present data suggested that it is necessary to pass a phased step so that the escape mutant against the anti-V3 antibody can emerge. Neutralization escape variants with V2 mutations in gp120 could be selected at relatively low KD-247 pressures, but high concentrations of KD-247 were required for induction of a completely resistant variant with amino acid substitution in the epitope. Moreover, we present evidence suggesting that some V2 mutations change the tertiary or quaternary structure of the envelope trimers on the viral surface that are involved in the neutralization resistance of the primary isolate. Clarification of the mechanisms responsible for this neutralization resistance may provide important insight into possible methods for the induction of potent and cross-neutralizing antibody responses capable of neutralizing various primary isolates.

(This work was presented in part at the 13th Conference on Retroviruses and Opportunistic Infection, Denver, CO, 5 to 8 February 2006 [55a].)

MATERIALS AND METHODS

Cells, culture conditions, reagents, and viruses. PM1/CCR5 cells (68) were maintained in RPMI 1640 medium (Sigma) supplemented with 10% heat-inactivated fetal calf serum (FCS; HyClone Laboratories, Logan, UT), 50 U/ml of penicillin, 50 mg/ml of streptomycin, and 100 μg/ml of G418 (Sigma). 293T cells were maintained in Dulbecco's modified Eagle medium (Sigma) supplemented with 10% heat-inactivated FCS. The CD4- and CCR5-expressing human osteogenic sarcoma cell line GHOST-hi5 was maintained in Dulbecco's modified Eagle medium supplemented with 10% FCS, G418 (200 μg/ml), hygromycin B (100 μg/ml; Sigma), and puromycin (1 μg/ml; Sigma).

KD-247, an anti-gp120-V3 antibody, was produced as previously described (11). 17b, a monoclonal antibody against the CD4-induced epitope, and immunoglobulin Gb12 (IgGb12), a monoclonal antibody against the CD4-binding epitope, were provided by the National Institutes of Health AIDS Research and Reference Reagent Program. 447-52D, an anti-gp120 V3 MAb, was a gift from Suzan Zolla-Pazner (New York University School of Medicine). 2D7, an anti-CCR5 MAb, and RPA-T4, an anti-CD4 MAb, were purchased from BD Biosciences Pharmingen (San Jose, CA). Human rsCD4 was purchased from R&D Systems, Inc. (Minneapolis, MN). TAK-779, a CCR5 inhibitor, was kindly provided by Takeda Chemical Industries, Ltd. (Osaka, Japan). AK-602, a CCR5 inhibitor, was gifted by Ono Pharmaceutical Co., Ltd. (Osaka, Japan).

The R5 primary HIV-1, MOKW virus, was isolated from a drug-naïve Japanese patient (36). This virus was passaged in phytohemagglutinin-activated peripheral blood mononuclear cells (PBMCs), and the culture supernatant was stored at −80°C until use.

Isolation of a KD-247-resistant mutant from MOKW virus in vitro. The selection of KD-247 escape variants from MOKW virus was performed as previously described (67). Briefly, MOKW virus was preincubated in the presence of KD-247 for 30 min at 37°C, and then PM1/CCR5 cells (4×10^4) were exposed to 500 times the 50% tissue culture infective dose ($TCID_{50}$) of the preincubated MOKW. After incubation for 5 h at 37°C, cells were pelleted down and resuspended in RPMI 1640 medium supplemented with 10% FCS without KD-247. Viral replication was monitored by observation of the cytopathic effects in PM1/CCR5 cells. The culture supernatant was harvested on day 7 and used to infect fresh PM1/CCR5 cells for the next round of culture in the presence of increasing concentrations of KD-247. When the virus began to propagate rapidly in the presence of KD-247, the MAb concentration was further increased. After the virus was passaged in the presence of up to 2,000 μg/ml KD-247 in PM1/CCR5 cells, a KD-247-resistant virus, MOKW9p(2000), was recovered from the cell culture supernatant. MOKW virus was also passaged for the same time period in PM1/CCR5 cells in the absence of KD-247, and the resulting virus was designated MOKW9p(−).

Amplification of viral cDNA and nucleotide sequencing. Viral RNA was extracted from cell culture supernatants with several concentrations of KD-247 using a QIAamp viral RNA kit (QIAGEN). Viral RNAs were reverse transcribed using a High Capacity cDNA Archive Kit (Applied Biosystems) with specific antisense primer ENVN (5′-CTGCCAATCAGGGAAGTAGCCTTGT GT-3′). Nested PCR was performed to amplify the gp120 C1 to C4 coding region as described previously (60). The primers used were as follows: for the first-step PCR, 1B (5′-AGAAAGAGCAGAAGACAGTGGCAATGA-3′) and H (5′-TA GTGCTTCCTGCTGCTCCCAAGAACCC-3′); for the second-step PCR, 2B (5′-AGCAGAAGACAGTGGCAATGAGAGTGA-3′) and F (5′-ATATAATT CACTTCTCCAATTGTCCCTCAT-3′). The products of the nested PCR were inserted in the TA vector (Invitrogen) and sequenced using a Big Dye Terminator, version 1.1 (Applied Biosystems), in accordance with the manufacturer's instructions.

MTT assay. The neutralization-sensitivities of each passaged MOKW virus to KD-247 were determined as previously described (67). Briefly, PM1/CCR5 cells (2×10^3 cells/well) were exposed to 100 $TCID_{50}$ of each passaged virus in the presence of various concentrations of KD-247 in 96-well round-bottom microculture plates and incubated at 37°C for 7 days. After removal of 100 μl of medium from each well, 10 μl of MTT (3-[4,5-dimethylthiazol-2-yl]-2,5-diphenyl tetrazolium bromide) solution (7.5 mg/ml) in phosphate-buffered saline (PBS) was added to each well, and the plate was incubated at 37°C for 3 h. After incubation, 100 μl of acidified isopropanol containing 4% (vol/vol) Triton X-100 was added to each well to dissolve the formazan crystals. The optical density (wavelength, 570 nm) was measured using a microplate reader. Assays were performed in duplicate or triplicate.

Construction of mutant envelope expression vectors. Proviral DNA was extracted from each batch of passaged MOKW virus-infected PM1/CCR5 cells using a QIAamp DNA blood mini kit (QIAGEN). For the construction of each passaged envelope expression vector, we used pCXN2, which has a chicken actin promoter. Briefly, we amplified MOKW gp160 regions using LA *Taq* (Takara) with primers ENVA (5′-GGCTTAGGCATCTCCTATGGCAGGAAGAA-3′) and ENVN (see above). The products of the PCR were inserted into pCR-XL-TOPO (Invitrogen). The sequences of the amplified *env* region of MOKW virus were confirmed using an ABI377 automated DNA sequencer. The EcoRI fragment of pCR-XL-MOKW containing the entire *env* region was ligated into pCXN2 to give pCXN-MOKW-RDP (the last three letters of the MOKW virus

constructs represent the amino acids at positions 166, 167, and 175 in the V2 region), pCXN-MOKW-KNL/C3m, and pCXN-MOKW-KNL/V3m. The pCXN-MOKW-KNL vector was constructed by replacing the StuI-Bsu36I fragment of pCXN-MOKW-KNL/C3m with a corresponding MOKW-RDP fragment. The pCXN-MOKW-RDP/V3m and pCXN-MOKW-RDP/C3m vectors were constructed by replacing the StuI-Bsu36I fragment of pCXN-MOKW-RDP with the corresponding pCXN-MOKW-KNL/V3m or pCXN-MOKW-KNL/C3m fragments, respectively. pCXN-MOKW-KNP, pCXN-MOKW-RDL, pCXN-MOKW-KDL, and pCXN-MOKW-RNL were generated by site-directed mutagenesis using a QuickChange Site-Directed Mutagenesis Kit (Stratagene) in accordance with the manufacturer's instructions.

Pseudovirus preparation. Five micrograms of pNL4-3.luc.R$^-$E$^-$ and 0.5 μg of pRSV-Rev (18), supplied by the NIH AIDS Research and Reference Reagent Program, and 4.5 μg of the MOKW Env-expressing pCXN2 were cotransfected into 293T cells using Effectene transfection reagent (QIAGEN). At 24 h after the transfection, the pseudovirus-containing supernatants were harvested, filtered through a 0.2-μm-pore-size filter, and stored at −80°C. To measure the pseudovirus activity, a luminescence assay using GHOST-hi5 cells was used as previously described (60).

Neutralization assays. A single-cycle infectivity assay was used to measure the neutralization of MOKW pseudoviruses as described previously (60). Briefly, MAbs at various concentrations and a pseudovirus suspension corresponding to 100 $TCID_{50}$ were preincubated on ice for 15 min. The virus-antibody mixtures were added to GHOST-hi5 cells, which on the preceding day had been seeded in a 96-well plate (1.5×10^4 cells/well). Cultures were incubated for 2 days at 37°C, washed with PBS, and lysed with lysis buffer (Luc PGC-50; PicaGene). Following transfer of the cell lysates to luminometer plates (Coastar 3912), the luciferase activity (in relative light units) in each well was measured using luciferase substrate (100 μl/well; PicaGene) in a TR717 microplate luminometer (Applied Biosystems). The reduction in infectivity was determined by comparing the relative light units in the presence and absence of MAbs and was expressed as the percentage of neutralization. The same assay was repeated two to three times.

In vitro binding assay to the MOKW envelope-expressing cell surfaces. In vitro binding assays were performed as previously described (53, 67). EcoRI fragments of MOKW *env* genes from pXL-MOKWs were subcloned into the corresponding sites in pDNR-1r (Clontech). The vectors were sequenced to confirm the presence of the desired *env* gene and the absence of other changes. The *env* gene fragments were then subcloned into pLP-IRES2-EGFP (Clontech) using Cre-recombinase (Clontech) in accordance with the manufacturer's instructions. 293T cells were cotransfected with pRSV-Rev (0.5 μg) and pLP-IRES2-EGFP-MOKW (9.5 μg) using the Effectene transfection reagent. After 36 h, the cells were harvested, incubated with each anti-HIV-1 MAb in combination with biotin-conjugated anti-human IgG and peridinin chlorophyll protein-conjugated streptavidin (BD Pharmingen), gated for the green fluorescent protein (GFP)-positive area, and analyzed using a FACSCalibur flow cytometry system.

MAb-gp120 binding assay. Culture supernatants containing the pseudotyped viruses were treated with 1% nonionic Nonidet P-40 to provide a source of gp120. Binding assays for MAbs to gp120 were then performed essentially as described elsewhere (41, 59). Briefly, gp120 proteins from transfected culture supernatants, diluted in Tris-buffered saline containing 10% FCS and 1% Nonidet P-40, were captured onto solid phase via their carboxyl termini using sheep polyclonal antibody D7324 (Aalto Bioreagents, Dublin, Ireland). MAb was added in PBS containing 10% FCS and 0.1% nonionic detergent Tween 20, and bound MAb was detected with alkaline phosphatase-conjugated goat anti-human IgG (Sigma) followed by the addition of phosphatase substrate (Sigma). A_{405} measurements were taken using a microplate reader.

Construction of chimeric NL4-3/MOKW *env* proviruses. Chimeric proviruses were constructed from the pNL4-3 proviral plasmid (AIDS Research and Reference Reagent Program, National Institute of Allergy and Infectious Diseases) by overlapping PCR as previously described, with minor modifications (31). Briefly, the gp160 coding sequences were amplified from the cloning vectors using the primers EnvFv (5′-AGCAGAAGACAGTGGCAATGAGAGCGAAG-3′) and EnvR (5′-TTTTGACCACTTGCCACCCATCTTATAGC-3′). A portion of the NL4-3 provirus from nucleotides 5284 to 6232 was amplified with primers NL(5284)F (5′-GGTCAGGGAGTCTCCATAGAATGGAGG-3′) and NL(6232)Rv (5′-CTTCGCTCTCATTGCCACTGTCTTCTGCT-3′). This fragment encompasses the unique EcoRI restriction site in pNL4-3. Another fragment from the NL4-3 provirus spanning nucleotides 8779 to 9045 was amplified using the primers NL(8779)F (5′-GCTATAAGATGGGTGGCAAGTGGTCAAAA-3′) and NL(9045)R (5′-GATCTACAGCTGCCTTGTAAGTCATTGGTC-3′). This fragment includes the unique XhoI restriction site in pNL4-3. Overlapping PCR was used to join the gp160 coding sequence from the desired clone to the fragment encompassing bases 8779 to 9045 that had been amplified from pNL4-3. The resulting fragment was then similarly joined to the amplified fragment encompassing bases 5284 to 6232 from pNL4-3. The product was digested with EcoRI and XhoI and subcloned into the corresponding site in pBluescript SK(+) (Stratagene) for sequencing and subsequent manipulation. The EcoRI-XhoI fragment for each *env* gene was then subcloned back into pNL4-3. The results were proviral plasmids that differed from each other only in the *env* gene. The resulting plasmids were designated pNL-MOKW-RDL and pNL-MOKW-KNL.

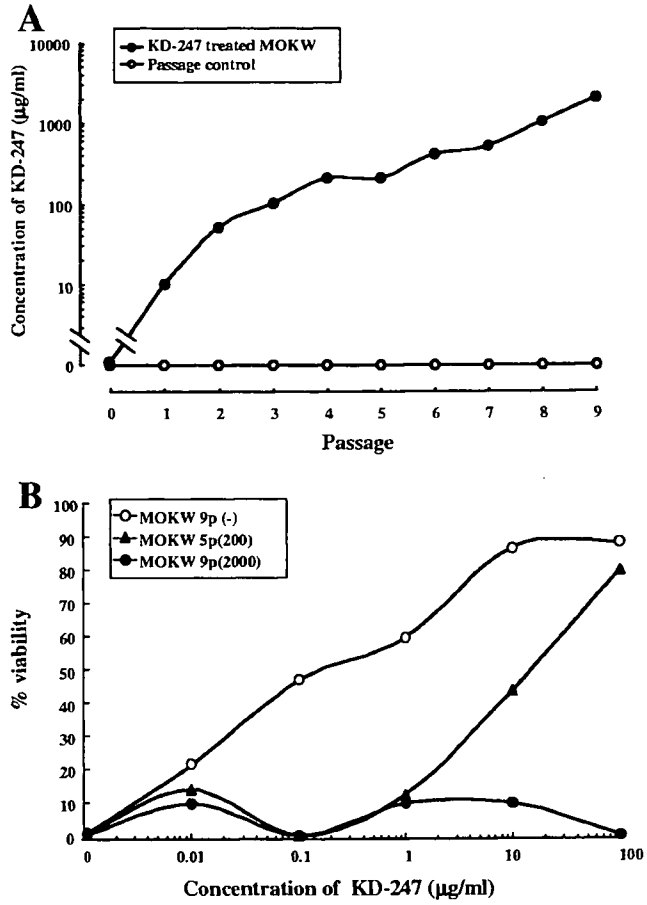

FIG. 1. Selection of neutralization-resistant virus variants against KD-247. (A) The selection was carried out in PM1/CCR5 cells, as described in Materials and Methods. (B) Sensitivity of MOKW5p(200) and MOKW9p(2000) virus to KD-247 as determined by MTT assay. PM1/CCR5 cells (2×10^3) were exposed to 100 $TCID_{50}$ of MOKW9p(−), MOKW5p(200), or MOKW9p(2000) virus and were cultured in the presence of various concentrations of KD-247. The IC_{50} values were determined by MTT assay on day 7 of culture. The assay was conducted in duplicate. The values shown are representative of three separate experiments.

Virus preparation and viral replication assay in PM1/CCR5 cells. Three micrograms of pNL-MOKW-RDL or pNL-MOKW-KNL was transfected into 293T cells using the Effectene transfection reagent. At 24 h after transfection, the virus-containing supernatants were harvested, filtered through a 0.2-μm-pore-size filter, and frozen in aliquots at −150°C. Viral yields were quantified by a RETROtek HIV-1 p24 antigen enzyme-linked immunosorbent assay (ELISA) kit (ZeptoMetrix). PM1/CCR5 cells (1×10^4) were exposed to NL4-3/MOKW *env* chimeric viruses corresponding to 10 ng of p24 and then preincubated for 4 h at 37°C. After incubation, cells were pelleted down and resuspended in RPMI 1640 medium supplemented with 10% FCS. Viral replication was monitored by measuring p24 kinetics in duplicate.

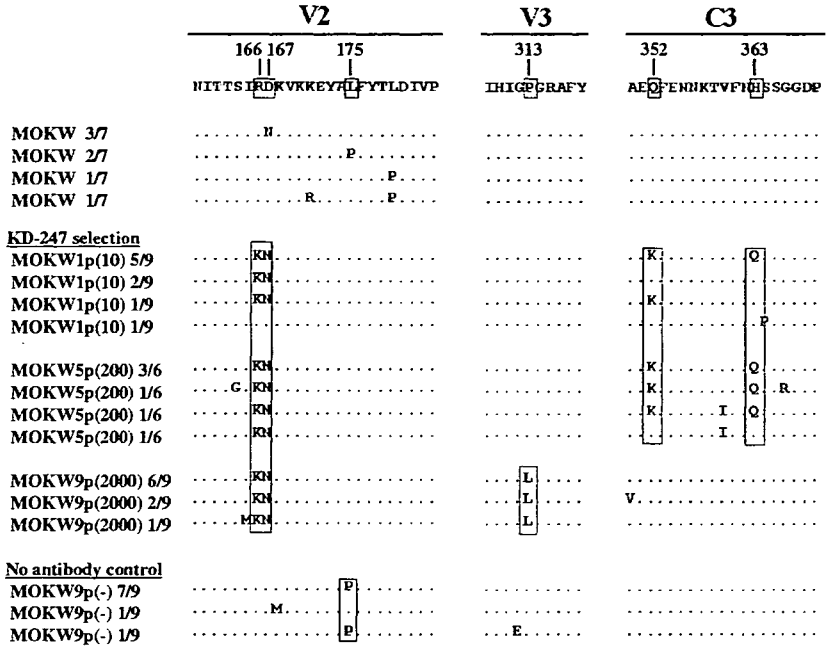

FIG. 2. Amino acid sequences of gp120 from the supernatants of MOKW-infected PM1/CCR5 cells passaged in the presence or absence of KD-247. Viral RNA from the cell culture supernatants at several concentrations of KD-247 was reverse transcribed. After the obtained cDNAs were subjected to PCR amplification and cloning, the *env* regions in the viruses passaged in the presence or absence of KD-247 were sequenced. The V2, V3, and C3 regions are indicated. The top amino acid sequence represents one of the major sequences from supernatants of MOKW-infected PBMCs. The locations and numbers of specific amino acids, based on the HXB2 sequence, are shown above the consensus line. The number of clones with the listed sequence among the total number of clones tested is given after each designation. For each set of clones, the deduced amino acid sequence of the gp120 was aligned by the single amino acid code. Dots denote sequence identity.

Nucleotide sequence accession numbers. Nucleotide sequences have been deposited in the DNA Data Bank of Japan under accession numbers AB262847 to AB262951 (passaged samples) and AB262952 to AB262961 (*env* expression vectors).

RESULTS

Anti-HIV-1 activity of KD-247 for the primary R5 isolate, MOKW virus. KD-247 recognized an epitope that contains the IGPGR sequence located at the tip of V3 and neutralized primary HIV-1 in clade B with matching sequence motifs (11). To study how bulked primary R5 virus can escape from anti-V3 antibody, we selected a genetically heterogenous HIV-1 primary isolate, MOKW, rather than a molecular clone to allow escape mutants to be selected from a quasi-species pool as well as to be generated de novo. MOKW virus was isolated by standard PBMC culture from a drug-naïve Japanese patient infected with HIV-1 by heterosexual contact (36). The isolate was sensitive to neutralization by KD-247 with a 50% inhibitory concentration (IC_{50}) of 3.4 μg/ml, which is comparable to the IC_{50} values of the Ba-L, JR-FL, and 89.6 viruses (data not shown).

Selection of KD-247 escape mutants from MOKW virus. To select an HIV-1 variant that could escape neutralization by KD-247 in vitro, we exposed PM1/CCR5 cells to MOKW virus and serially passaged the virus in the presence of increasing concentrations of KD-247. PM1/CCR5 cells were highly sensitive to both X4 and R5 HIV infection and were accompanied by prominent syncytia (68). As a control, MOKW virus was passaged under the same conditions but without KD-247 to allow us to monitor spontaneous changes that occurred in the virus during prolonged PM1/CCR5 cell passaging. The selected virus was initially propagated in the presence of 10 μg/ml KD-247, and during the course of the selection procedure, the MAb concentration was increased to 2,000 μg/ml (Fig. 1A). After five rounds of passaging, a viral variant, designated MOKW5p(200), arose that replicated in the presence of 200 μg of KD-247 per ml. Moreover, after nine rounds of passaging, a viral variant, designated MOKW9p(2000), arose that infected PM1/CCR5 cells efficiently in the presence of 2,000 μg/ml KD-247 (Fig. 1A). We harvested each passaged virus and a passaged control virus, designated MOKW9p(−), and evaluated their sensitivity to KD-247 using the MTT assay (Fig. 1B). The IC_{50} values of KD-247 against the MOKW9p(−), MOKW5p(200), and MOKW9p(2000) viruses were 0.15 μg/ml, 16 μg/ml, and >100 μg/ml, respectively, indicating that MOKW virus had acquired a resistance phenotype against KD-247 during the in vitro selection.

Sequences of the envelope region of the KD-247 escape mutants. To determine the genetic basis underlying the resistance of the variant MOKW strains, the *env* gene was amplified and sequenced. The C1 to C4 regions of the envelope were sequenced after cloning the PCR product for each region using cDNAs synthesized from viral RNAs obtained from the supernatants of infected cells, as previously described (67). A total of six to nine clones for each sample from PCR products from the passaged viruses were isolated and sequenced.

Before selection by KD-247 was begun, the V2 regions of MOKW *env* had variable amino acid sequences (Fig. 2). In

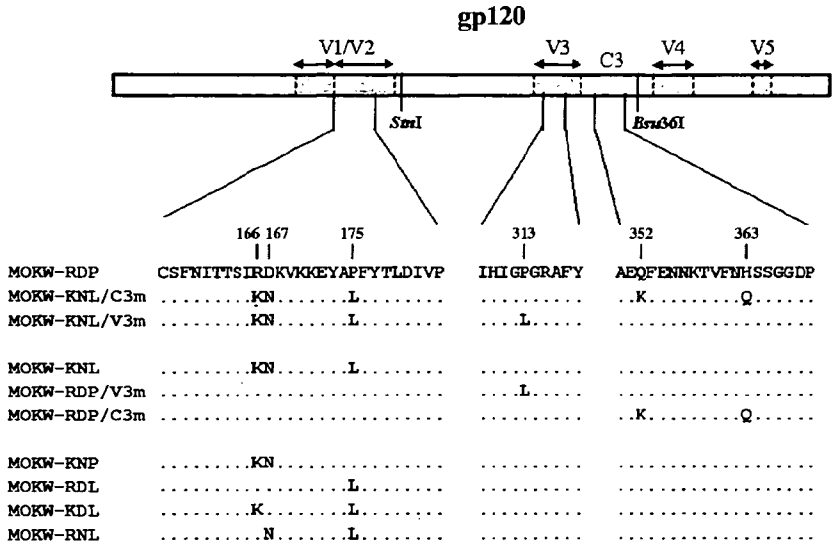

FIG. 3. Schematic representation of recombinant MOKW *env* genes used for analysis of the genetic basis for resistance to KD-247. MOKW-RDP, MOKW-KNL/C3m, and MOKW-KNL/V3m *env* genes were amplified from passaged MOKW virus-infected PM1/CCR5 cells in the absence or presence of KD-247. MOKW-KNL, MOKW-RDP/V3m, and MOKW-RDP/C3m *env* genes were constructed by replacing each region of MOKW-RDP with the corresponding MOKW-KNL/C3m or MOKW-KNL/V3m sequence. MOKW-KNP, MOKW-RDL, MOKW-KDL, and MOKW-RNL viruses were constructed by site-directed mutagenesis. Construction of the clones and mutagenesis procedures are described in Materials and Methods. The locations and numbers of specific amino acids, based on the HXB2 sequence, are shown above the MOKW-RDP sequence.

the first passage, two amino acid mutations in the V2 region and two amino acid mutations in the C3 region (five of nine clones) appeared, and after the fifth passage, the ratios of V2 and C3 mutated variants had further increased (seven of eight clones). However, after the ninth passage, the C3 mutations had completely disappeared, and a Pro-to-Leu substitution (P313L) in the V3 tip emerged in addition to the mutations in the V2 region (Fig. 2). The appearance of escape mutants with a V3 tip mutation was anticipated, because prior studies on the profile of KD-247 binding to peptides suggested that amino acid substitution at the V3 tip abrogates MAb binding (11). Some changes in the envelope sequence in other regions, including C1, V1, C2, V4, and C4, of the escape mutant were found even at early time points in the presence of the selective pressure. It is possible that these mutations also confer resistance to KD-247 but lead to viruses with decreased fitness, and thus they did not expand in the subsequent passage (Fig. 2 and data not shown). The virus passaged in PM1/CCR5 cells without KD-247 did not show the P313L substitution at passage 9 (zero of nine clones) (Fig. 2). However, accumulation of a mutation of leucine to proline at position 175 (L175P) in the V2 region was observed in the culture without KD-247. This mutation was not found in any passaged variants with KD-247.

Neutralization sensitivities of mutated MOKW pseudoviruses. To determine which substitutions were responsible for KD-247 resistance, we constructed luciferase-reporter viruses which were pseudotyped with the representative envelopes of MOKW5p(200), MOKW9p(2000), and passaged viruses without KD-247 [MOKW9p(−)], and were designated MOKW-KNL/C3m, MOKW-KNL/V3m, and MOKW-RDP virus, respectively (Fig. 3). Chimeric envelopes were constructed by replacing the mutated-region (V2, V3, or C3) with a corresponding MOKW-RDP virus (designated MOKW-KNL, MOKW-RDP/V3m, and MOKW-RDP/C3m, respectively), and then sensitivity was compared with that of the passaged virus without KD-247. As shown in Fig. 4, the V3-tip-mutated pseudoviruses, MOKW-KNL/V3m and MOKW-RDP/V3m, were completely resistant to KD-247 (>25,000-fold), whereas V2-mutated viruses, MOKW-KNL/C3m and MOKW-KNL, were only partially resistant (125-fold and 500-fold, respectively) (Fig. 4 and Table 1). The involvement in neutralization resistance of mutation in the V1/V2 region has been reported by number of researchers (12, 49, 50, 54). Our results show that the MOKW variants that had V2 mutations and a resistance phenotype against KD-247 were selected under pressure from relatively low concentrations of KD-247 (10 to 200 μg/ml) and that evolution of fully resistant variants with a mutation in the V3 tip was observed under pressure from high concentrations of the antibody.

We then determined whether the KD-247 escape variants remained sensitive to other neutralizing antibodies (447-52D and 17b), rsCD4, anti-CCR5 antibody (2D7), anti-CD4 antibody (RPA-T4), and the small-molecule CCR5 inhibitor (TAK-779) (Fig. 4 and Table 1). The KD-247 escape variants with the P313L mutation, MOKW-KNL/V3m and MOKW-RDP/V3m, were also resistant to another anti-V3 MAb, 447-52D, and V2-mutated viruses without V3 mutation, MOKW-KNL/C3m and MOKW-KNL, were partially resistant (the same as for KD-247). In contrast, the V2-mutated viruses (MOKW-KNL/C3m, MOKW-KNL/V3m, and MOKW-KNL) showed resistance to rsCD4 and 17b (a MAb to the CD4-induced epitope; CD4i) compared with the pseudoviruses without V2 mutations, i.e., MOKW-RDP, MOKW-RDP/C3m, and MOKW-RDP/V3m. Moreover, the pseudoviruses with V3 tip mutations, MOKW-KNL/V3m and MOKW-RDP/V3m, be-

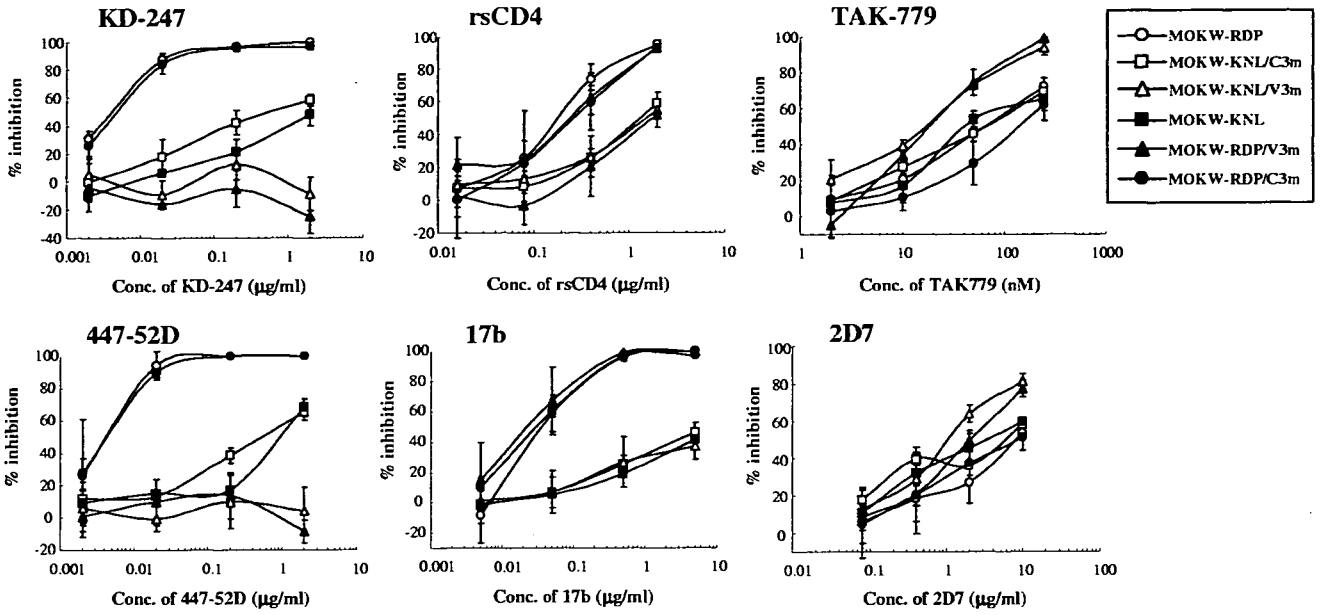

FIG. 4. Neutralization sensitivities of pseudoviruses with *env* genes from passaged MOKW viruses to MAbs, rsCD4, and CCR5 inhibitors. Pseudoviruses with the envelope sequences listed on the figure were prepared as described in Materials and Methods. KD-247, 447-52D, rsCD4, and 17b were preincubated with 100 $TCID_{50}$ of each MOKW pseudotype virus for 15 min, followed by the addition of the mixtures to the target cells (GHOST-hi5). The target cells were treated with TAK-779 and 2D7 for 15 min, followed by inoculation of the pseudotype clones. The inhibitory effects were determined by measuring the luciferase activities on day 2 of culture. Conc, concentration.

came significantly more sensitive to TAK-779 and 2D7 compared with pseudoviruses without the P313L mutation (Fig. 4 and Table 1). No significant differences with respect to sensitivity to RPA-T4 were observed between any pseudoviruses (Table 1). These data indicate that V3 tip and V2 mutations confer neutralization resistance against anti-V3 antibodies and that these mutations affect viral sensitivity to neutralizing antibodies recognizing different epitopes and anti-CCR5 antibody/agents.

Binding affinity of neutralizing antibodies to MOKW Env proteins on the cell surface. To elucidate the mechanism by which escape virus variants with V3 tip and V2 mutations become less sensitive to neutralizing antibodies, MOKW Env-expressing 293T cells were established by transfection with each Env expression plasmid and then stained with the MAbs. Binding of KD-247, 447-52D, and 17b to the surface-expressed Env proteins was assayed using fluorescence-activated cell sorter (FACS) analysis. As shown in Fig. 5A, the mean fluorescence intensities (MFIs) of KD-247 binding to the Env proteins without either V2 or V3 mutations (the MOKW-RDP and MOKW-RDP/C3m cells) were 30.13 and 29.20, respectively. However, the corresponding values for the V3-tip-mutated Env-expressing cells (MOKW-KNL/V3m and MOKW-RDP/V3m) were almost the same as negative controls (6.90 and 6.66, respectively). The MFI of the V2-mutated Env-expressing cells (MOKW-KNL/C3m and MOKW-KNL) indicated a lower binding affinity (17.89 and 19.18, respectively) than for Env proteins without V2 and V3 mutations. The binding pattern of 447-52D to these Env-expressing cells was similar to that of KD-247 (Fig. 5B). However, reduction in the binding of 17b was observed for strains with V2-mutated Env proteins (MOKW-KNL/C3m, MOKW-KNL/V3m, and

TABLE 1. Anti-HIV-1 activities of various MAbs and inhibitors toward MOKW pseudoviruses

Class	Compound	IC_{50} (μg/ml) of the indicated virus (relative IC_{50})[a]					
		MOKW-RDP	MOKW-KNL/C3m	MOKW-KNL/V3m	MOKW-RDP/C3m	MOKW-KNL	MOKW-RDP/V3m
V3 MAbs	KD-247	0.004 (1)	0.5 (125)	>100 (>25,000)	0.005 (1.3)	2 (500)	>100 (>25,000)
	447-52D	0.004 (1)	0.5 (125)	>2 (>500)	0.004 (1)	0.8 (200)	>2 (>500)
CD4-induced MAb	17b	0.035 (1)	>5 (>143)	>5 (>143)	0.03 (0.86)	>5 (>143)	0.02 (0.57)
CD4	rsCD4	0.18 (1)	1.3 (7.22)	1.5 (8.33)	0.24 (1.33)	1.8 (10)	0.24 (1.33)
CCR5 MAb	2D7	8 (1)	6.8 (0.85)	1 (0.13)	8 (1)	3.2 (0.4)	2 (0.25)
CCR5 inhibitor	TAK-779	63 (1)	63 (1)	18 (0.29)	140 (2.22)	65 (1)	18 (0.29)
CD4 MAb	RPA-T4	0.4 (1)	0.26 (0.65)	0.22 (0.55)	0.5 (1.25)	0.22 (0.55)	0.44 (1.1)

[a] GHOST-hi5 cells were exposed to 100 $TCID_{50}$ of each MOKW pseudovirus and then cultured in the presence of various concentrations of MAb or inhibitors. The IC_{50} values were determined using the luciferase reporter assay on day 2 of culture. All assays were conducted in triplicate. The value in parentheses is the ratio of the IC_{50} of the compound to the IC_{50} of the MOKW-RDP virus. Values for the compound TAK-779 are nanomolar concentrations. Data shown are representative of two or three separate experiments.

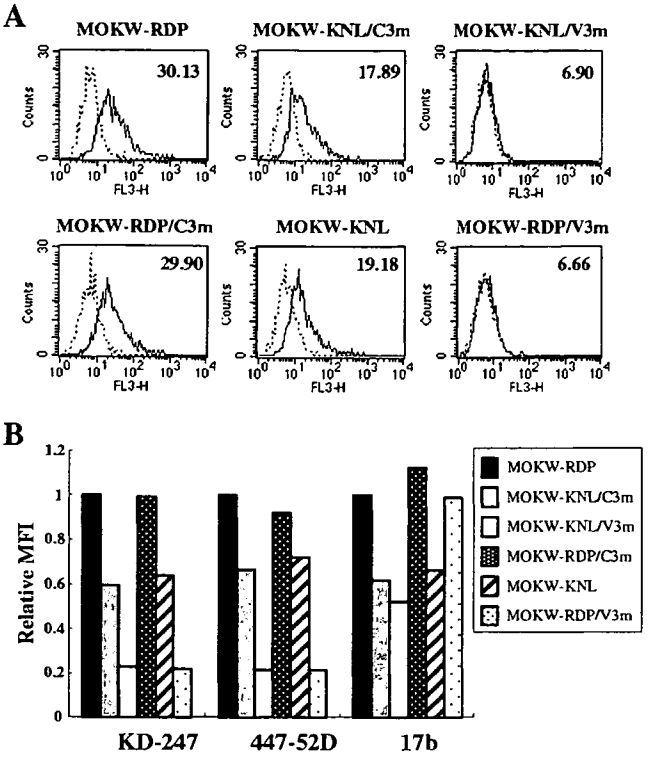

FIG. 5. Comparison of antibody binding to cell surface-expressed MOKW Env proteins. (A) 293T cells transfected with MOKW Env expression vectors were harvested at 24 h posttransfection and stained with KD-247. Flow cytometry data for binding of the KD-247 (black lines) to cell surface MOKW Env proteins are shown among GFP-gated 293T cells along with the control antibody (normal human IgG; dotted lines). The number at the top right of each graph is the MFI. (B) Each bar indicates the relative binding of KD-247, 447-52D, and 17b to MOKW Env-expressing cell surfaces. Data were normalized to each antibody's MFI for MOKW-RDP virus. FL3-H, relative fluorescence.

MOKW-KNL), whereas no difference in 17b binding was noted for the V3-mutants without V2 mutations (Fig. 5B). These findings are consistent with the results of a single-round neutralization assay (Fig. 4). Taken together, these data suggest that the mutations in V2 have a significant influence on access by antibodies to V3 as well as to the CD4i epitope. This is because access by antibodies to the epitopes of the functional envelope is related to neutralization sensitivity or resistance.

Identification of the V2 region site responsible for the neutralization resistance phenotype by site-directed mutagenesis of specific residues. Because KD-247 recognizes an epitope containing the IGPGR amino acid sequence in the V3 tip, the MAb could not bind the V3 tip of mutated Env proteins. Consequently, KD-247 does not neutralize V3-tip-mutated virus strains (67). However, the mechanism of neutralization resistance associated with V2 mutations is not known. To clarify the responsible mutation in the V2 region that confers the escape phenotype with respect to KD-247, we introduced V2 amino acid changes individually and in combination into the MOKW-RDP Env expression vector (Fig. 3) and measured the sensitivities of pseudoviruses with these envelopes to KD-247. As shown in Fig. 6, the R166K/D167N double mutant, MOKW-KNP virus, showed almost the same neutralization sensitivity as MOKW-RDP virus against KD-247. Surprisingly, a single amino acid change (P175L in MOKW-RDL) was sufficient to confer >10,000-fold resistance upon MOKW-RDP virus, with an IC_{50} of >100 μg/ml. R166K/P175L (MOKW-KDL) mutations also conferred resistance. Both the MOKW-RDL and MOKW-KDL viruses were much more resistant than the fully V2-mutated virus, MOKW-KNL (>100-fold and >10-fold resistance, respectively) (Fig. 6). The D167N/P175L (MOKW-RNL) mutant was more resistant than MOKW-KNL virus (10-fold) but less resistant than the MOKW-RDL and MOKW-KDL viruses. We also constructed a V2 mutant of JR-FL and confirmed that JR-FL with an amino acid substitution of Leu to Pro at position 175 became highly sensitive to KD-247 compared with JR-FL with Leu at position 175 in Env (data not shown). These results suggest that residue 175 (Pro or Leu) is the crucial amino acid for determining neutralization sensitivity against KD-247 and that the phenotypic influence of the R166K and D167N changes is strictly context dependent, requiring the presence of Leu at residue 175.

We then determined whether these pseudoviruses with various V2 mutations remained sensitive to other neutralizing antibodies (447-52D and IgGb12), rsCD4, 2D7, RPA-T4, and TAK-779 (Fig. 6). MOKW-RDL and MOKW-KDL viruses were also resistant to another anti-V3 MAb, 447-52D, CD4 binding site MAb, IgGb12, and rsCD4. MOKW-RNL was partially resistant compared with MOKW-KNL but less resistant than MOKW-RDL and MOKW-KDL against 447-52D, IgGb12, and rsCD4. These results were similar to those for KD-247. All V2-mutated clones were sensitive to TAK-779 and 2D7, as was MOKW-RDP virus (Fig. 6 and data not shown). However, the anti-CD4 MAb RPA-T4 neutralized both the MOKW-RDL and MOKW-KDL viruses at an approximately threefold lower concentration than other viruses (Fig. 6). These results suggest that the amino acids at positions 166 and 167 (with RD and KN sequences) may help compensate for any reduced fitness of viruses with Leu at residue 175. On the other hand, Pro at position 175 in MOKW-RDP virus might be accumulated because it confers better fitness to replicate on PM1/CCR5 cells in the absence of KD-247 pressure.

Binding affinity of MAbs against monomeric or cell surface-expressed gp120 with mutations in V2. To determine the difference in binding of MAbs to monomeric gp120 of MOKW Env with V2 mutations relative to that of MOKW-RDP virus, we performed MAb binding assays. Monomeric gp120 was prepared from pseudoviruses that had a series of V2 mutations and was captured on an ELISA plate, followed by detection by MAbs. No difference was noted in the binding activity of KD-247 or 447-52D to monomeric gp120 from V2-mutated and MOKW-RDP envelopes (Fig. 7). These results suggest that V2-mutated Env proteins retain the neutralizing epitope at least in monomeric gp120.

In contrast to the monomeric form, gp120 expressed on the cell surface contained, to a certain degree, functional envelope oligomers that were directly related to the infectivity and neutralization sensitivity of the virus. To compare the binding activity of MAbs for the surface-expressed Env with the results obtained for monomeric gp120, 293T cells transfected with MOKW-RDP and MOKW-KNP viruses, a V2 mutant strain, were subjected to FACS analysis. As shown in Fig. 8A and B,